



Late Weichselian and Holocene palaeoceanography of Storfjordrenna, southern Svalbard

M. Łącka¹, M. Zajączkowski¹, M. Forwick², and W. Szczuciński³

¹Institute of Oceanology, Polish Academy of Sciences, Powstańców Warszawy 55, 81-712 Sopot, Poland

²Department of Geology, University of Tromsø – The Arctic University of Norway, 9037 Tromsø, Norway

³Institute of Geology, Adam Mickiewicz University in Poznań, Maków Polnych 16, 61-606 Poznań, Poland

Correspondence to: M. Łącka (mlacka@iopan.gda.pl)

Received: 15 July 2014 – Published in Clim. Past Discuss.: 1 August 2014

Revised: 22 January 2015 – Accepted: 26 February 2015 – Published: 27 March 2015

Abstract. Multiproxy analyses (including benthic and planktonic foraminifera, $\delta^{18}\text{O}$ and $\delta^{13}\text{C}$ records, grain-size distribution, ice-rafted debris, XRF geochemistry and magnetic susceptibility) were performed on a ^{14}C -dated marine sediment core from Storfjordrenna, located off of southern Svalbard. The sediments in the core cover the termination of Bølling–Allerød, the Younger Dryas and the Holocene and reflect general changes in the oceanography/climate of the European Arctic after the last glaciation. Grounded ice of the last Svalbard–Barents Sea Ice Sheet retreated from the coring site ca. 13 950 cal yr BP. During the transition from the subglacial to glaciomarine setting, Arctic Waters dominated the hydrography in Storfjordrenna. However, the waters were not uniformly cold and experienced several warmer spells. A progressive warming and marked change in the nature of the hydrology occurred during the early Holocene. Relatively warm and saline Atlantic Water began to dominate the hydrography starting from approximately 9600 cal yr BP. Although the climate in eastern Svalbard was milder at that time than at present (smaller glaciers), two periods of slight cooling were observed in 9000–8000 and 6000–5500 cal yr BP. A change in the Storfjordrenna oceanography occurred at the beginning of the late Holocene (i.e. 3600 cal yr BP) synchronously with glacier growth on land and enhanced bottom current velocities. Although cooling was observed in the Surface Water, Atlantic Water remained present in the deeper portion of the water column of Storfjordrenna.

1 Introduction

The northward flowing North Atlantic Current (NAC) is the most important source of heat and salt in the Arctic Ocean (Gammelsrod and Rudels, 1983; Aagaard et al., 1987; Schauer et al., 2004; Fig. 1b). The main stream of Atlantic Water (AW) flowing north to Fram Strait in the form of the West Spitsbergen Current (WSC) causes a dramatic reduction of the sea-ice extent and thickness via the warming of the intermediate water layer in this region of the Arctic Ocean (Quadfasel et al., 1991; Serreze et al., 2003). Palaeoceanographic (e.g. Spielhagen et al., 2011; Dylmer et al., 2013) and instrumental (Walczowski and Piechura 2006, 2007; Walczowski et al., 2012) investigations provide evidence of a recent intensification of the flow of AW in the Nordic Seas and the Fram Strait.

The Svalbard archipelago is influenced by two water masses: AW flowing northward from the North Atlantic and Arctic Water (ArW) flowing southwest from the northern Barents Sea (Fig. 1b). An oceanic front arising at the contact of different bodies of water is an excellent area for research of contemporary and past environmental changes. Intensification of AW flow and associated climate warming result in decreased sea-ice cover in the Svalbard fjords during winter (Berge et al., 2006) and an increased sediment accumulation rate (Zajączkowski et al., 2004; Szczuciński et al., 2009) and influence the pelage–benthic carbon cycling (Zajączkowski et al., 2010).

Palaeoceanographic records indicate that AW was present along the western margin of Svalbard, at least during the last 12 000 years (e.g. Ślubowska-Woldengen et al., 2007;

Werner et al., 2011; Rasmussen et al., 2013), and occasionally reached the Hinlopen Trough and Kvitøya Trough, thus transporting warmer and more saline water to the eastern portion of Svalbard from the north (Ślubowska-Woldengen et al., 2007; Ślubowska-Woldengen et al., 2008; Kubischta et al., 2010; Klitgaard Kristensen et al., 2013). Periods of enhanced inflow of AW during the Holocene led to the expansion of marine species that are absent or only rarely occurring at present. These species include the mollusc *Mytilus edulis* whose fossil remains are widely distributed in raised beach deposits on the western and northern coasts of Svalbard (e.g. Feyling-Hanssen and Jørstad, 1950; Hjort et al., 1992). *Mytilus edulis* spawn at temperatures above 8–10 °C (Thorarinsdóttir and Gunnarson, 2003) and thus are considered to indicate higher surface-water temperature related to stronger AW inflow during the early Holocene (11 000–6800 cal yr BP) (Feyling-Hanssen, 1955; Salvigsen et al., 1992; Hansen et al., 2011). Although the progressive development of *Mytilus edulis* is well documented by periods of warming and inflow of AW to the Hinlopen Trough, the presence of this species in Storfjorden (W Edgeøya; Fig. 1) is unclear. Hansen et al. (2011) suggested that a small branch of warm AW could have reached eastern Spitsbergen from the south at that time.

In the 1980s and 1990s, Storfjorden was thought to be exclusively influenced by the East Spitsbergen Current (ESC), which carries cold and less saline ArW from the Barents Sea (Quadfasel et al., 1988; Piechura et al., 1996). More recent studies suggested that the hydrography in Storfjorden is affected by the production of brine-enriched shelf waters (e.g. Haarpaintner et al., 2001; Rasmussen and Thomsen, 2009), the creation of a coastal polynya (e.g. Skogseth et al., 2005; Geyer et al., 2010) or the overflow of dense waters to the continental shelf (e.g. Fer et al., 2003). However, hydrological data obtained from conductivity–temperature sensors attached to a *Delphinapterus leucas* showed a substantial and topographically steered inflow of AW to Storfjorden through the Storfjordrenna (Lydersen et al., 2002). Recently, Aki-mova et al. (2011) reviewed typical water masses for Storfjorden, where the AW was located between 50 and 70 m.

Storfjordrenna is a sensitive boundary area (Fig. 1) where two contrasting water masses form an oceanic polar front separating the colder, less saline and isotopically lighter ArW from warmer, highly saline and $\delta^{18}\text{O}$ -heavier AW. An abrupt cooling (e.g. Younger Dryas, Little Ice Age) and warming (e.g. early Holocene warming) of the European Arctic might be linked to relatively small displacements of this front (Sarnthein et al., 2003; Hald et al., 2004; Rasmussen et al., 2014, 2015).

Two sediment cores collected at the mouth of Storfjordrenna reveal a continuous inflow of AW to the southwestern Svalbard shelf since the deglaciation of Svalbard–Barents Ice Sheet (Rasmussen et al., 2007), whereas the inner Storfjorden basins underwent a shift from occupation by continental ice to an ice proximal condition (Rasmussen and Thomsen,

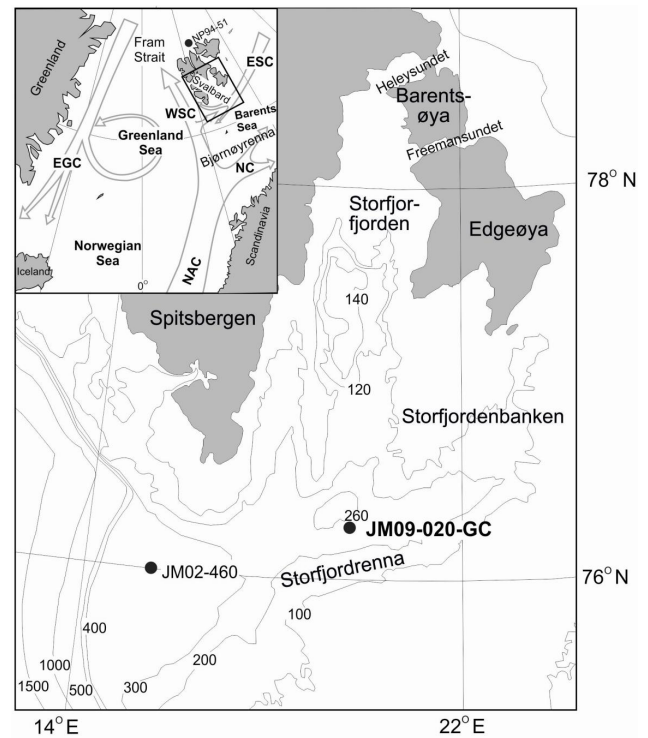


Figure 1. Location map (a) showing the core site from this study (JM09-020-GC) and core site of JM02-460 (Rasmussen et al., 2007). The inset map (b) shows the modern surface oceanic circulation in Nordic Seas and location of a core NP94-51 (Ślubowska et al., 2005). Abbreviations: NAC: Norwegian–Atlantic Current; WSC: West Spitsbergen Current; ESC: East Spitsbergen Current; EGC: East Greenland Current; NC: Norwegian Current. The cores JM02-460 and NP94-51 are discussed in the text.

2014, 2015). Nevertheless, a limited amount of palaeoceanographical data are available from this region, and thus the reconstruction of the Svalbard–Barents Ice Sheet retreat and the further development of Storfjordrenna oceanography are often speculative.

In this paper, we present results from multi-proxy analyses of a sediment core retrieved 100 km east of the mouth of Storfjordrenna (Fig. 1a). We provide a new age for the retreat of the last Svalbard–Barents Sea Ice Sheet from Storfjordrenna and discuss the interaction of oceanography and deglaciation as well as the postglacial history of Atlantic Water inflow onto the shelf off of southern Svalbard. Because the studied sediment core was retrieved from an oceanographic frontal zone, which is sensitive to larger-scale changes, we believe that the presented data show the general climatic/oceanographic trends in the eastern Arctic.

2 Oceanographic setting

Storfjorden is an approximately 190 km long and up to 190 m deep glacial trough located between the landmasses of Spits-

bergen to the west, Edgeøya and Barentsøya to the east, and the shallow Storfjordenbanken to the southeast (Fig. 1a). It is not a fjord *sensu stricto* because the sounds of Heleysundet and Freemansundet to the north and northeast, respectively, connect the head of Storfjorden to the northwestern Barents Sea. A sill of 120 m depth crosses the mouth of Storfjorden. The 254 km long Storfjordrenna, a continuation of the trough that extends towards the shelf break, is located beyond this sill. The bottom depth along the trough axis varies between 150 and 420 m (Pedrosa et al., 2011).

The water column of Storfjorden and Storfjordrenna is composed of two main water masses transported with currents from the east and south and mixed waters that are formed locally (Table 1 after Skogseth et al., 2005). Warm and saline AW enters Storfjordrenna in a cyclonic manner (Schauer, 1995; Fer et al., 2003), flowing into the trough parallel to its southern margin and flowing towards the trough mouth along its northern slope. The AW occurs between 50 and 70 m in Storfjorden and extends to a depth of 200 m in Storfjordrenna (Akimova et al., 2011). The origin of AW entering Storfjordrenna is an eastward branch of the North Atlantic Current (NAC) following the topography of the Barents Sea Shelf Break. However, approximately 50 % of the AW flowing northward also penetrates into Bjørnøyrenna (Smedsrud et al., 2013; for location, see Fig. 1). The AW in Storfjordrenna is cooler and fresher than in Bjørnøyrenna as an effect of the distance and mixing processes (O'Dwyer et al., 2001). The AW may occasionally propagate even further east of Svalbard, where it fills depressions below 180 m (Schauer, 1995). Relatively cold ArW is transported to Storfjorden and Storfjordrenna by the ESC. The ESC enters the fjord through the tidally influenced sounds of Heleysundet and Freemansundet in the north and northeast (Norges Sjøkartverk, 1988) as well as from the southeast with a coastal current flowing near Edgøya (Loeng, 1991). The AW and ArW mix to form Transformed Atlantic Water (TAW), which dominates on the shelf off of West Spitsbergen (Svendsen et al., 2002; Table 1). Dense, brine-enriched Shelf Water (BSW) in Storfjorden is produced through high polynya activity and results from intense formation of sea-ice (Haarpaintner et al., 2001; Skogseth et al., 2004, 2005). The BSW fills the fjord to the top of the sill (120 m) and initiates a gravity-driven overflow (Quadfasel et al., 1988; Schauer, 1995; Schauer and Fahrback, 1999; Fer et al., 2003, 2004; Skogseth et al., 2005). The BSW is characterised by a salinity value greater than 34.8 and a temperature at or slightly above the freezing point (Table 1). Surface Water (SW) in the upper 50 m is cold and fresh during the autumn and warm and fresh during the summer due to ice melting. In winter, the water column in Storfjorden is homogenised due to wind and tidal mixing and is considered to have a temperature close to the freezing point (Skogseth et al., 2005).

Table 1. Water mass characteristics in Storfjorden and Storfjordrenna (Skogseth et al., 2005, modified). The two main water masses are in bold.

Water mass names	Water mass characteristics	
	Temperature (°C)	Salinity
Atlantic Water (AW)	>3.0	>34.95
Arctic Water (ArW)	<0.0	34.3–34.8
Brine-enriched Shelf Water (BSW)	< −1.5	> 34.8
Surface Water (SW)	> 0.0	< 34.4
Transformed Atlantic Water (TAW)	> 0.0	> 34.8

3 Materials and methods

Multi-proxy analyses of the gravity core JM09-020-GC provided the foundation for this study. The core was retrieved with R/V *Jan Mayen* (University of Tromsø – The Arctic University of Norway, UiT) in November 2009 from the Storfjordrenna (76°31489' N, 19°69957' E) at a bottom depth of 253 m (Fig. 1a). The coring site was located in an area above the continuous presence of BSW and was selected after an echo-acoustic investigation to identify the greatest possible area of flat bottom with a minimum disturbance of sediments. Conductivity–temperature–depth (CTD) measurements were performed prior to coring (Fig. 2a) and in summer 2013 (Fig. 2b).

Prior to sediment core opening, the magnetic susceptibility (MS) was measured using a loop sensor installed on a GEOTEK Multi Sensor Core Logger at the Department of Geology, UiT. Core sections were stored in the laboratory for one day prior to measurements, thus allowing the sediments to adjust to room temperature and avoiding measurement errors related to temperature changes (Weber et al., 1997). The X-radiographs and digital images were collected from half of the core to define the sedimentary and biogenic structures. The sediment colour was defined according to the Munsell Soil Color Charts (Munsell Products, 2009). Qualitative element geochemical measurements were performed with an Avaatech X-ray fluorescence (XRF) core scanner using the following settings: 10 kV, 1000 µA, 10 s measuring time, and no filter. Both core halves were subsequently cut into 1 cm slices and transported to the Institute of Oceanology at the Polish Academy of Sciences in Sopot for further analyses.

Sediment samples for foraminiferal analyses were freeze-dried, weighed, and wet sieved using sieves with mesh sizes of 500 and 100 µm. The residues were dried, weighed again and subsequently split on a dry micro-splitter. Where possible, at least 300 specimens of foraminifera were counted in every 5 cm of sediment. Species identification under a binocular microscope (Nikon SMZ1500) was supported using the classification of Loeblich and Tappan (1987), with few exceptions, and percentages of the eight indicator species were

applied. The number of species per sample and Shannon–Wiener index were calculated using the program Primer 6. The benthic foraminiferal abundance and ice-rafted debris (IRD; grains > 500 μm) were counted under a stereomicroscope and expressed as flux values (number of specimens/grains $\text{cm}^{-2} \text{ka}^{-1}$) using the bulk sediment density and sediment accumulation rate.

Stable oxygen and carbon isotope compositions of tests of the infaunal foraminifer species *Elphidium excavatum* f. *clavata* were determined at the Department of Geological Sciences, University of Florida (Florida, USA). All values are calibrated to the Pee Dee Belemnite (PDB) scale and corrected for ice volume changes. In our study, we discuss the $\delta^{18}\text{O}$ and $\delta^{13}\text{C}$ record as a relative measure for changes in the water mass characteristics (temperature–salinity) and/or the supply of meltwater/freshwater to the area. Moreover, no reliable vital effect correction has been created for *E. excavatum* f. *clavata* (Bauch et al., 2004; Ślubowska-Woldengen et al., 2007), and therefore we did not correct the isotopic values for vital effect.

Grain size (< 2 mm) analyses were performed every 1 cm using a Malvern Mastersizer 2000 laser particle analyser and presented as volume percent. To examine the relative variability in the near-bottom currents, the mean grain-size distribution of the < 63 μm fraction was calculated to avoid the effect of ice-rafted coarse fraction. The mean grain size was calculated using the program GRADISTAT 8.0 according to the geometric method of moments (Blott and Pye, 2001).

The chronology for this study is based on high-precision AMS ^{14}C measurements of fragments from nine calcareous bivalve shells. Measurements were performed in the Poznań Radiocarbon Laboratory, which is equipped with a 1.5 SDH-Pelletron Model “Compact Carbon AMS” (Czernik and Goslar, 2001; Goslar et al., 2004). The surface layer of shells was scraped off to avoid contamination with younger carbonate encrustation. The AMS ^{14}C dates were converted into calibrated ages using the calibration program CALIB 6.1 (Stuiver and Reimer, 1993; Stuiver et al., 2005) and the Marine13 calibration curve (Reimer et al., 2013). The difference ΔR in reservoir age correction of the model ocean and region of Svalbard was reported by Mangerud et al. (2006) as 105 ± 24 or 111 ± 35 , and we used the first value. The calibrated ages are presented in Table 2. It should be noted that the reservoir age is based on a few data points from western Spitsbergen, and the age may be different for the eastern coast. However, no data are available from the latter region.

4 Results

4.1 Modern hydrology

In November 2009, the SW at the coring site (upper ~ 27 m) had already cooled (1.24°C ; Fig. 2a); however, its salinity was still low (34.24). Transformed AW was observed in the

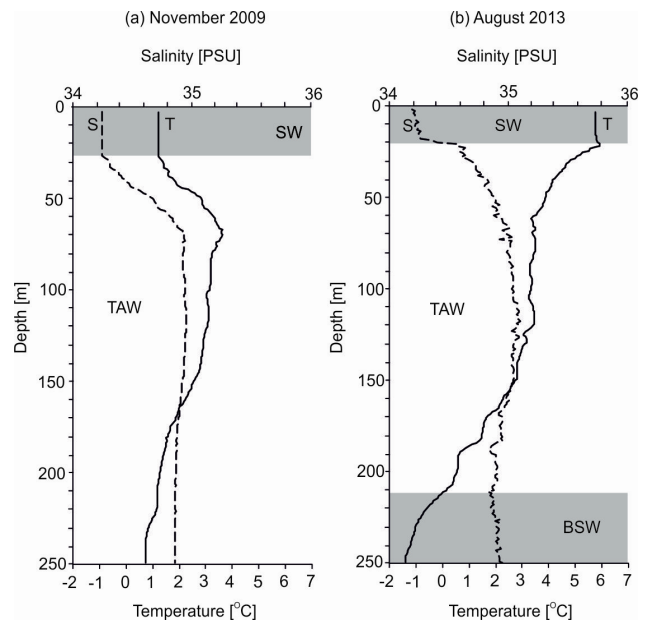


Figure 2. Temperature and salinity versus depth, measured on 5 November 2009 (a) and on 13 August 2013 (b) at the site of core JM09-020GC. SW: Surface Water, TAW: Transformed Atlantic Water, BSW: Brine-enriched Shelf Water.

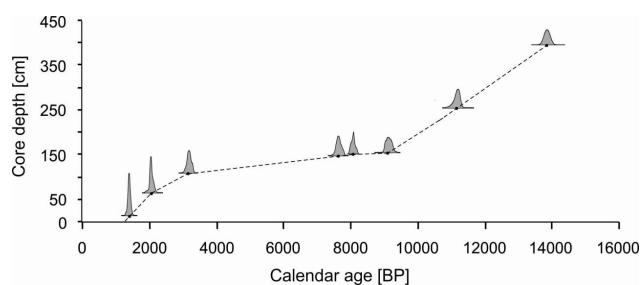
layer between 60 and 160 m. The lowermost portion of the water column shows evidence of gradual cooling that reached a minimum temperature of 0.76°C near the bottom. The lack of BSW at the bottom indicates gradual water mixing during summer and fall. In August 2013, the SW had a slightly lower salinity, but the temperature was $\sim 5^\circ\text{C}$ higher than in November 2009 (Fig. 2b). The TAW occupied the same depths as in 2009. However, an almost 50 m thick layer of BSW was present close to the seafloor.

4.2 Age model

The ^{14}C ages and calibrated ages are reported in Table 2. The calibration gives an age distribution and not a single value; thus, the 2-sigma range is presented, and Fig. 3 shows the age probability distribution curves. The ages of the samples generally increase with sediment depth except in the case of one sample, namely St 20A 39, which provided an older age than the sample below. That shell was most likely re-deposited and thus was not used for the age model. However, because all of the samples used for dating were shell fragments, it must be noted that it is possible that more samples could be subjected to re-deposition, but based on the available data, it is not possible to confirm. The age model is based on the assumption of linear sediment accumulation rates between data points. The highest probability peaks from the calibrated age ranges were used as input values for the model. For the lowermost and uppermost regions of the core, we adopted sediment accumulation rates for the neighbouring region. It

Table 2. AMS ^{14}C dates and calibrated ages.

Sample No	Depth (cm)	Lab No	Raw AMS ^{14}C BP	Calibrated years BP $\pm 2\sigma$	Cal yr BP used in age model	Dated material
St 20A 5/6	5	Poz-46955	1835 \pm 30	1200–1365	1285	<i>Ciliatocardium ciliatum</i>
St 20A 39	38.5	Poz-46957	2755 \pm 30	2245–2470	Not used	<i>Astarte crenata</i>
St 20 78/79	78	Poz-46958	2735 \pm 30	2177–2429	2320	<i>Astarte crenata</i>
St 20 110	109.5	Poz-46959	3450 \pm 30	3079–3323	3220	<i>Astarte crenata</i>
St 20 142	141.5	Poz-46961	6580 \pm 40	6850–7133	6970	<i>Astarte crenata</i>
St 20A 152	151.5	Poz-46962	7790 \pm 40	8018–8277	8160	<i>Astarte crenata</i>
St 20 157	156.5	Poz-46963	8610 \pm 50	8989–9288	9120	<i>Bathyrca glacialis</i>
St 20 251/252/253	252	Poz-46964	10 200 \pm 60	10 895–11 223	11 230	<i>Thracia</i> sp.
St 20 396	395.5	Poz-46965	12 570 \pm 60	13 780–14 114	13 950	Bivalvia shell

**Figure 3.** Age–depth relationship for JM09-020-GC based on eight AMS ^{14}C calibrated ages with 2-sigma age probability distribution curves. The chronology is established by linear interpolation between the calibrated ages.

is common to observe the loss of the sediment surface layer during coring with heavy gravity cores. In the case of core JM09-020-GC, it is likely that at least the top 40 cm of sediments were lost during coring. This conclusion is supported by analysis of a box corer collected prior to coring (Łącka et al., 2015). The extrapolated age model for the sediment surface is therefore 1200 cal yr BP.

4.3 Sedimentological and geochemical parameters

The core JM09-020-GC is 426 cm long and consists of four lithological units: L1 (bottom of the core to 370 cm; > 13 450 cal yr BP), L2 (370–272 cm; ~ 13 450 to ~ 11 500 cal yr BP), L3 (272–113 cm; ~ 11 500 to ~ 3600 cal yr BP) and L4 (113 cm to core top; ~ 3600 to ~ 1200 cal yr BP). The lithological log was created based on the X-radiographs, grain-size analysis data and foraminiferal flux (Fig. 4). Grains > 2 mm are referred to as “clasts” and are marked in the lithological logs as individual features.

Unit L1 consists of compacted massive dark grey (5Y 4/1) sandy mud with various amounts of clasts. Bioturbation and foraminifera were generally absent. However, one shell fragment was found at approximately 395 cm.

Unit L2 contains massive dark grey (5Y 4/1) sandy mud with an amount of coarser material and generally lower amounts of clasts than unit L1. The mean grain size (< 63 μm) ranged from 7 to 10 μm . The highest IRD flux and Fe/Ca ratio for the entire core occur in this unit. The mass accumulation rate (MAR) is 0.043 $\text{g cm}^{-2} \text{yr}^{-1}$. The first signs of bioturbation occur in this unit, and the flux of foraminifera increases rapidly up to ~ 5700 individuals $\text{cm}^{-2} \text{ka}^{-1}$ (Fig. 4).

The unit L3 is composed of massive dark olive grey mud (5Y 3/2) and is characterised by decreasing MAR values (0.019–0.002 $\text{g cm}^{-2} \text{yr}^{-1}$), moderate sand content and clearly increasing mean grain size (< 63 μm). The IRD flux is low, and the Fe/Ca ratio decreases gradually until ca. 9200 cal yr BP and remains low (between 3 and 4; Fig. 4). Continuous bioturbation and variable foraminiferal fluxes are observed, with maxima in the intervals 9000–8000 and 6000–5500 cal yr BP.

The uppermost unit L4 is primarily composed of the same material as the underlying unit, i.e. massive dark olive grey mud (5Y 3/2). However, the sand content is occasionally higher. The MAR increases to 0.024 $\text{g cm}^{-2} \text{yr}^{-1}$. The mean grain size (< 63 μm) throughout this interval is even higher than that in L3 and reaches up to 15 μm ; the Fe/Ca ratio is increasing. The bioturbation continues, numerous shell fragments are present, and the foraminifera flux reaches high values throughout the entire unit.

4.4 Foraminiferal fauna

A total of 54 calcareous and six agglutinated species were identified. The foraminiferal assemblages were dominated by calcareous fauna. Agglutinated species occurred only in 14 sediment samples, and their abundance did not exceed 4%. The only exception is the sample dated to ca. 11 350 cal yr BP (262.5 cm depth) with 25% of agglutinated foraminiferal fauna. However, in this sample, the total foraminifera abundance was low (13 specimens g^{-1} sediment). In general, species richness, number of agglutinated foraminifera, and

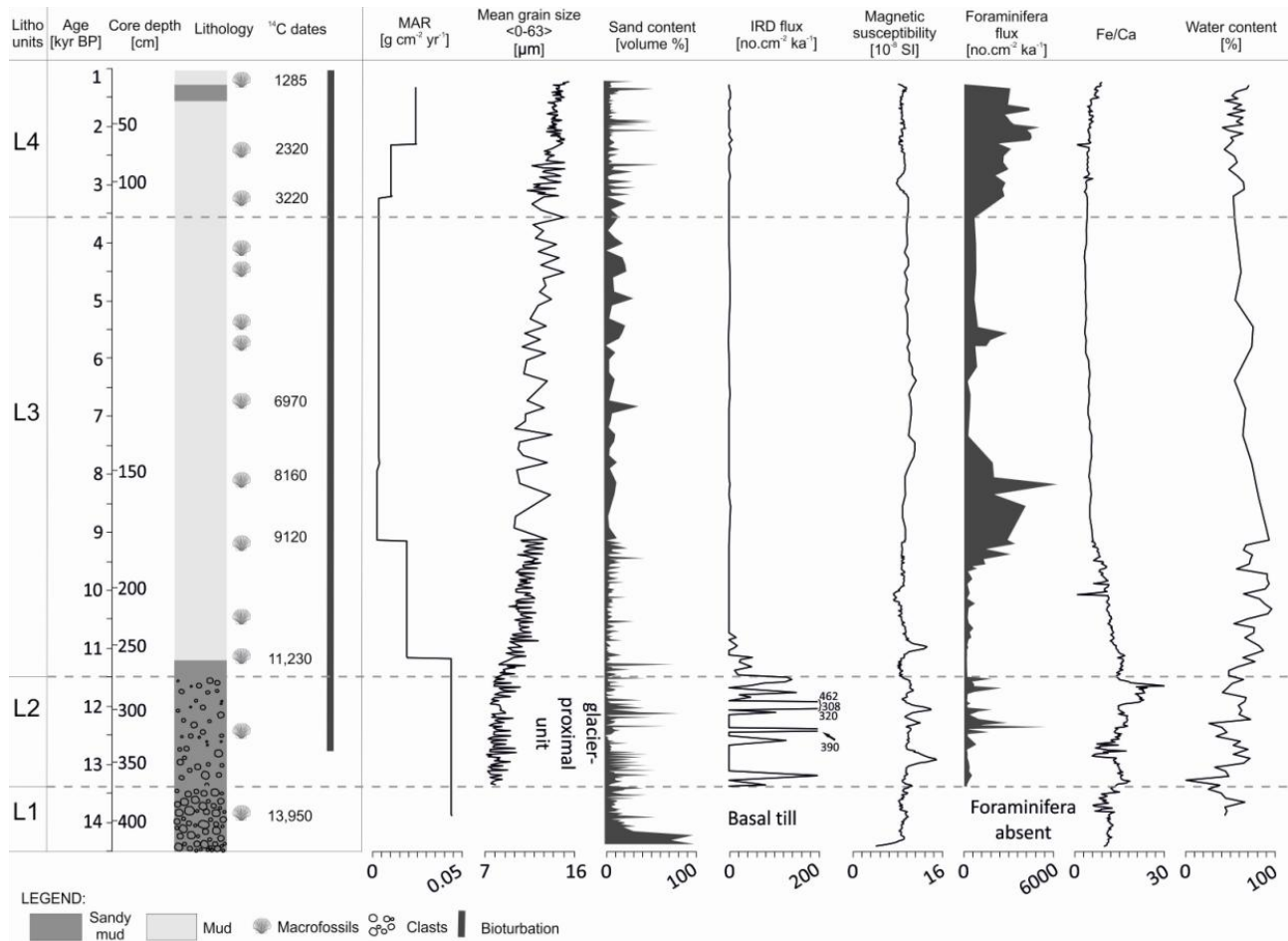


Figure 4. Lithological log of core JM09-020GC. Lithology, ^{14}C dates, occurrence of bioturbation, mass accumulation rates, mean grain size in the range of 0–63 μm , sand content, ice-rafted debris flux, magnetic susceptibility, foraminifera flux as well as Fe/Ca ratio and water content. The results are presented with lithostratigraphic units (L1–L4), versus calendar years (cal kyr BP) and core depth (cm).

rare and fragile species increase towards the top of the core. Benthic foraminiferal fauna is dominated by *Elphidium excavatum* f. *clavata*, *Cassidulina reniforme*, *Nonionella labradorica*, *Melonis barleeanum*, *Islandiella* spp. (*Islandiella norcrossi*/*Islandiella helenae*) and *Cibicides lobatulus*. Percentages of *E. excavatum* f. *clavata* show an inverse relationship to *C. reniforme* with the almost constant dominance of the latter species in the periods $\sim 12\,450$ to $\sim 12\,000$ cal yr BP and $\sim 9\,600$ to $\sim 2\,800$ cal yr BP (Fig. 5). Planktonic foraminifera are represented by three species: *Neogloboquadrina pachyderma* (sinistral), *Neogloboquadrina pachyderma* (dextral) and *Turborotalita quinqueloba*. However, the two latter species are quite rare. In general, the abundance of planktonic fauna is low in the older portions of the core and slightly increases at approximately 10 000 cal yr BP, reaching maximum values ca. 2000 cal yr BP (Fig. 5).

Based on the most significant changes in the foraminiferal species abundances, species diversity, and $\delta^{18}\text{O}$ and $\delta^{13}\text{C}$ in *E. excavatum* f. *clavata* tests, the core was divided into four

foraminiferal zones F1–F4: $\sim 13\,450$ – $11\,500$ cal yr BP (F1); $11\,500$ – $9\,200$ cal yr BP (F2); $9\,200$ – $3\,600$ cal yr BP (F3); and $3\,600$ – $1\,200$ cal yr BP (F4) (Fig. 5). The zones correspond to lithological divisions. The age of unit F4 is the same as L4, units F3 and F2 correspond to L3, and unit F1 is linked to unit L2. In unit L1, foraminifera are rare to absent.

Zone F1 is dominated by the opportunistic *E. excavatum* f. *clavata* and *C. reniforme*. The latter species dominates more than *E. excavatum* f. *clavata* between 12 250 and 11 950 cal yr BP. High percentages of *C. lobatulus* (up to 57%) and *Astronion gallowayi* (up to 2.5%) occur occasionally. The planktonic foraminifera flux was low at the beginning of this section (mean value of nine specimens $\text{cm}^{-2} \text{ka}^{-1}$) and completely disappeared for nearly 1500 years from approximately 11 500 cal yr BP (Fig. 5). The species richness and the Shannon–Wiener index show low biodiversity compared with the upper portion of the core (mean values of 8 and 1.26, respectively). Furthermore, maxima of $\delta^{18}\text{O}$ and $\delta^{13}\text{C}$ occur in this interval.

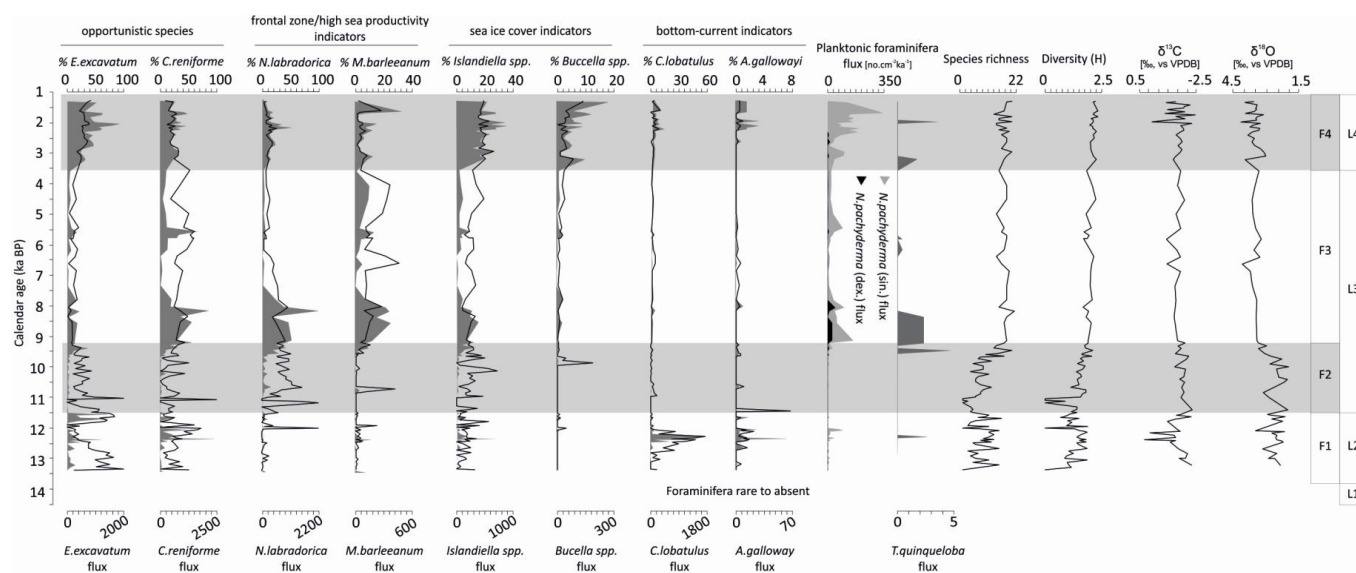


Figure 5. Percentage distributions (upper scale; black line) of the most dominant benthic species, fluxes (no. $\text{cm}^{-2} \text{ka}^{-1}$; bottom scale; grey shading) of benthic and planktonic foraminiferal species, diversity parameters (species richness and Shannon–Wiener index) and stable oxygen and carbon isotope data ($\delta^{18}\text{O}$ and $\delta^{13}\text{C}$) plotted versus thousands of calendar years with indicated foraminiferal zonation (zones F1–F4) and lithostratigraphic units (L1–L4). Foraminiferal taxa are grouped based on their ecological tolerances described in the text.

In zone F2, the contribution of *E. excavatum* f. *clavata* and *C. reniforme* is slightly lower, and *N. labradorica* becomes the most abundant species (Fig. 5). There is also an increase in *Islandiella* spp. percentage. Planktonic foraminifera appeared again ca. 10 000 cal yr BP. Biodiversity significantly increased, and $\delta^{18}\text{O}$ reached its minimum value of 2.61 ‰ vs. Vienna Pee Dee Belemnite at approximately 10 000 cal yr BP.

Zone F3 is characterised by the minimum mass accumulation rates of sediment and consequent low temporal resolution. *C. reniforme* dominates over *E. excavatum* f. *clavata* throughout. *M. barleeaanum* has its maximum abundance in this zone, and *N. labradorica* is abundant in the lower portions of this zone, decreasing at approximately 7000 cal yr BP. *Islandiella* spp. increases upcore. Planktonic foraminifera occur in the entire zone, and the fluxes are higher than those of previous units (Fig. 5). Biodiversity remains high in this zone, and $\delta^{18}\text{O}$ and $\delta^{13}\text{C}$ remain generally stable; however, marked peaks occurred at approximately 6800, 6500 and 5700 cal yr BP, respectively.

A consistently high foraminiferal flux of up to ~ 4900 specimens $\text{cm}^{-2} \text{ka}^{-1}$ characterises zone F4. The fluxes of *Islandiella* spp. and *Buccella* spp. increase significantly, and from 2850 cal yr BP, *Islandiella* spp. dominated the assemblage with *E. excavatum* f. *clavata*. Additionally, the fluxes of *C. lobatulus* and *A. gallowayi* increase; however, their abundances are lower than those of zone F2. A maximum abundance of planktonic foraminifera occurs in this unit. Foraminifera biodiversity continues to increase towards the core top (up to 2.33; Fig. 5), and $\delta^{18}\text{O}$ and $\delta^{13}\text{C}$ increase slightly with numerous fluctuations.

5 Discussion

The European Arctic includes continental slope strongly influenced by northward flowing Atlantic water and large shelf of the Barents Sea characterised by less saline and colder water. The available broad range of studies concerning palaeoceanography of the European Arctic focus on its marginal sites: westernmost (e.g. Rasmussen et al., 2007; Eldevik et al., 2014; Sternal et al., 2014), northern (Wollenburg et al., 2004; Klitgaard Kristensen et al., 2013) and eastern (Polyak and Solheim, 1994), while the border zone lying between the slope of continental shelf and central Barents Sea is poorly studied. The lack of well-defined and sufficiently complete palaeoceanographic record containing the signal from both of these environments encouraged the authors to study a sediment core retrieved inside Storfjordrenna, especially in the light of current hydrological changes in this area (e.g. Lydersen et al., 2002; Skogseth et al., 2005; Akimova et al., 2011). This location should present the general trends in the eastern Arctic, including Svalbard glacier activities, pack-ice in the Arctic Ocean and North Atlantic water circulation, moreover it avoids the local (fjordic) condition. We decided to discuss the presented record chronologically as a postglacial interplay between two hydrological regimes. Based on the most pronounced changes in sedimentological and foraminiferal data as well as comparisons with previous studies from adjacent areas, we distinguish five units in the studied core: a subglacial unit ($> 13\,450$ cal yr BP), a glacier-proximal unit (13 450–11,500 cal yr BP), a glaciomarine unit I (11 500–9200 cal yr BP), a glaciomarine unit II

(9200–3600 cal yr BP) and a glaciomarine unit III (3600–1200 cal yr BP).

5.1 Subglacial unit (> 13 450 cal yr BP)

The lowermost unit L1 (Fig. 4) was significantly coarser, more compacted and devoid of foraminifera, which indicates that it is likely of subglacial origin. During the late Weichselian Glacial Maximum, Storfjorden and Storfjordrenna were covered by an ice stream that drained the Svalbard–Barents Ice Sheet (SBIS; e.g. Ottesen et al., 2005). The SBIS deglaciation occurred as a response to the sea-level rise and increased mean annual temperature (Siegert and Dowdeswell, 2002). Rasmussen et al. (2007) noted that the outer portion of Storfjordrenna (389 m depth; Fig. 1a) was deglaciated prior to 19 700 cal yr BP. The bivalve shell fragment from 395.5 cm in our core suggests that the centre portion of Storfjordrenna was ice-free before ~13 950 cal yr BP. This observation indicates that the ~100 km long retreat of the grounding line from the shelf break to the central portion of Storfjordrenna occurred over approximately 5700 years. The deglaciation of the inner Storfjorden basin occurred ca. 11 700 cal yr BP (Rasmussen and Thomsen, 2014), whereas the coasts of the east Storfjorden islands, Barentsøya and Edgeøya, which are located over 100 km north from the coring site, occurred some 500 years later, i.e. 11 200 cal yr BP (recalibrated after Landvik et al., 1995). Siegert and Dowdeswell (2002) noted that during the Bølling–Allerød warming (ca. 14 700–12 700 cal yr BP), certain of the deeper bathymetric troughs (e.g. Bjørnøyrenna) had deglaciated first, and large embayments of ice formed around them. It is likely that Storfjordrenna was one of such embayments at that time. Our data are in agreement with ice stream retreat dynamics presented by Rütther et al. (2012) and refine the recent models of the Barents Sea deglaciation (e.g. Winsborrow et al., 2010; Hormes et al., 2013; Andreassen et al., 2014).

5.2 Glacier-proximal unit (13 450–11 500 cal yr BP)

The transition from a subglacial to glaciomarine setting is observed as a distinct change in sediment colour, several peaks of IRD, a decreased amount of clasts and the appearance of foraminifera. The sediment accumulation rate ($0.043 \text{ g cm}^{-2} \text{ yr}^{-1}$) was of the same order of magnitude as that of the modern proximal and central regions of the West Spitsbergen fjords (see Szczuciński et al., 2009 for a review). Textural and compositional analyses of L2 recorded a bimodal grain-size distribution and low abundance of microfossils, suggesting that deposition during the deglaciation occurred due to suspension settling from sediment-laden plumes and ice rafting (Lucchi et al., 2013; Witus et al., 2014). This unit in our core is limited to ~60 cm and is characterised by a lack of bioturbation in its lower portion.

The high flux of IRD is supported by the high Fe/Ca ratio and the depleted $\delta^{18}\text{O}$ values correlate well with the abundance of *C. lobatulus* and *A. gallowayi* (Figs. 4 and 5), two species connected with high-energy environments (Østby and Nagy, 1982), thus indicating that the coring site was likely located proximal to one or several ice fronts during the time of deposition of this unit.

During an early phase of the deglaciation of Storfjorden, the East Spitsbergen Current was still not active because the ice sheet grounded between Svalbardbanken and Storfjordbanken blocked the passage between eastern and western Svalbard (Rasmussen et al., 2007; Hormes et al., 2013). Thus, the first foraminiferal propagules (juvenile forms) were transported by sea currents (Alve and Goldstein, 2010) from the south and west and settled on the seafloor that was exposed after the retreat of grounded ice. The proximal glaciomarine environment affected the foraminiferal assemblages and resulted in low species richness, biodiversity and low foraminiferal abundance. Consequently, foraminifera assemblages became dominated by fauna typical of the glacier proximal settings: *E. excavatum* f. *clavata*, *C. reniforme* and *Islandiella* spp. (e.g. Vilks, 1981; Osterman and Nelson, 1989; Polyak and Mikhailov, 1996; Hald and Korsun, 1997). The dominance of *E. excavatum* f. *clavata* confirms the proximity to the ice sheet, decreased salinity and high water turbidity (e.g. Steinsund, 1994; Korsun and Hald, 1998; Włodarska-Kowalczyk et al., 2013).

The upper portion of unit L2 (ca. 12 800–11 500 cal yr BP) spans the Younger Dryas (YD) stadial. Records of marine sediments from Nordic and Barents Seas (e.g. Rasmussen et al., 2007; Ślubowska-Woldengen et al., 2007, 2008; Zamelczyk et al., 2012; Groot et al., 2014) as well as $\delta^{18}\text{O}$ records from Greenland ice cores (e.g. Dansgaard et al., 1993; Grootes et al., 1993; Mayewski et al., 1993; Alley, 2000) show that the YD was characterised by a rapid and short-term temperature decrease. This event was likely driven by the weakened North Atlantic Meridional Overturning Circulation, a result of the Lake Agassiz outburst (e.g. Gildor and Tziperman, 2001; Jennings et al., 2006; Murton et al., 2010; Cronin et al., 2012) or the interaction between the sea-ice and thermohaline water circulation (Broecker, 2006), which led to a reduction of AW transport to the north and a dominance of fresher Arctic Water. Our data show that the heavier $\delta^{18}\text{O}$ values recorded, e.g. 12 720 and 12 100 cal yr BP, correlate with reduced to absent IRD fluxes, whereas the peaks of lighter $\delta^{18}\text{O}$, e.g. 12 450, 12 150, and 11 780 cal yr BP, occurred synchronously with significant enhanced IRD fluxes (Fig. 6). The absence of IRD, occasionally for several decades, might reflect temporary polar conditions (Dowdeswell et al., 1998; Gilbert, 2000) characterised by the formation of perennial pack ice in Storfjorden that locked icebergs proximal to their calving fronts and prevented their movement over the coring site (Forwick and Voren, 2009). Wollenburg et al. (2004) observed a decrease in palaeoproductivity on the northern Barents Sea margin be-

tween 12 800 and 12 500 cal yr BP and the later palaeoproductivity peak at the termination of YD; they concluded that permanent sea-ice cover causes the decrease in sea productivity, whereas enhanced advection of Atlantic Water to the site might result in palaeoproductivity increase. Those periods of accelerated AW inflow resulted in massive iceberg rafting and delivery of IRD to Storfjordrenna, thus reflecting more sub-polar conditions. Hydrological variability during the Younger Dryas was previously noted in selected circum-North-Atlantic deep-water records (Bakke et al., 2009; Elmore and Wright, 2011 and references therein; Pearce et al., 2013). Moreover, oxygen stable isotope records from an ice-core GISP2 show certain warmer spells during that time (Stuiver et al., 1995), which coincides with higher ice rafting in Storfjordrenna (Fig. 6). Bakke et al. (2009) noted that the earlier portion of YD was colder and more stable, whereas the latter portion of this period was characterised by alternations between sea-ice cover and an influx of warmer and saltier North Atlantic waters. Our records show that during the late YD, the $\delta^{18}\text{O}$ data were slightly shifted towards lighter values. Temporal resolution of our records does not allow for more detailed comparison with available data; nevertheless, they clearly indicate that the Younger Dryas was not uniformly cold and that at least a number of warmer spells occurred on eastern Svalbard.

We also conclude that the data on $\delta^{18}\text{O}$ presented in Fig. 6 reflect temperature variations at the coring site according to the isotopically lighter ArW palaeotemperature model (Duplessy et al., 2005). Another explanation for the heavier $\delta^{18}\text{O}$ periods during the YD could be the intermittent inflow of warmer AW; however, this is unlikely to cause the synchronous disappearance of IRD.

5.3 Glaciomarine unit I (early Holocene; 11 500–9200 cal yr BP)

During the early Holocene, foraminiferal fauna, although low in abundance, were dominated by species related to the glaciomarine environment (*E. excavatum* and *C. reniforme*; Fig. 5). Increasing species richness and biodiversity of foraminifera point to amelioration of environmental conditions and a progressive increase in the distance to the glacier front (Korsun and Hald, 2000; Włodarska-Kowalczyk et al., 2013). The decrease of the Fe/Ca ratio is suggested to reflect increased the marine productivity and a reduced supply of terrigenous material (Croudace et al., 2006). The mean grain size ($> 63 \mu\text{m}$; Fig. 4) indicates weaker bottom currents at the beginning of the early Holocene and stronger bottom currents at the end of this period, which might be related to the ongoing isostatic uplift of the land masses of Svalbard as well as the sea level rise (e.g. Forman et al., 2004; Taldenkova et al., 2012).

Significant fluctuations of $\delta^{18}\text{O}$ and $\delta^{13}\text{C}$ and increasing abundance of *N. labradorica* and *Islandiella* spp. suggest that Storfjordrenna was under the influence of various water

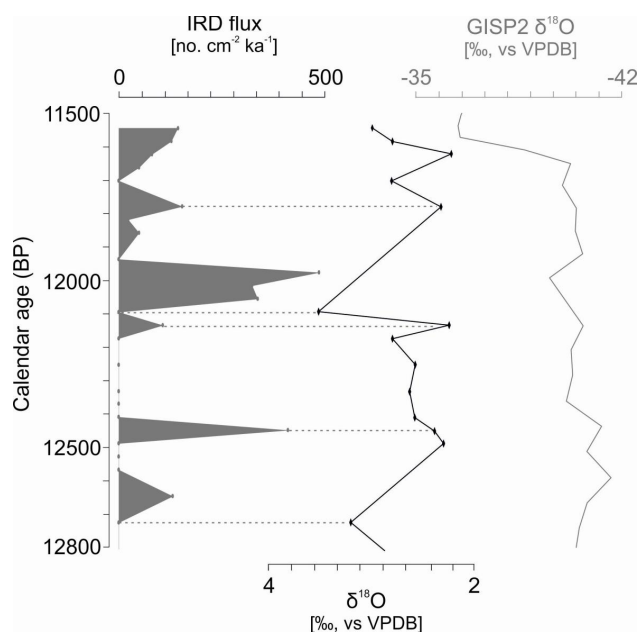


Figure 6. IRD flux (upper scale, grey shading) and oxygen stable isotopes records (bottom scale, black line) compared with oxygen stable isotope records from ice core GISP2 from Greenland during the Younger Dryas period (12 800–11 500 cal yr BP; Stuiver et al., 1995).

masses at this time (Fig. 5). Comparison of our $\delta^{18}\text{O}$ records with records from the Storfjorden shelf (400 m depth; Rasmussen et al., 2007; Fig. 1a) and the northern shelf of Svalbard (400 m depth; Ślubowska et al., 2005; Fig. 1b) shows that all of the records are shifted towards lighter values in the early Holocene (Fig. 7a), and the record from our core shows the most depletion (from ca. 13 000 cal yr BP). We suggest that the records located on the western and northern shelf of Svalbard directly mirror the effect of warmer Atlantic Water inflow, whereas records from Storfjordrenna were under the influence of isotopically lighter Arctic Water from the Barents Sea (Duplessy et al., 2005). The shift from the Arctic Water domain to the Atlantic Water domain during the end of the early Holocene is also visible on a scatter plot of $\delta^{13}\text{C}$ against $\delta^{18}\text{O}$ (Fig. 7b). The results grouped to the left indicate Arctic Water domination, whereas the results grouped to the right show Atlantic Water domination.

According to Kaufman et al. (2004), the early Holocene is characterised by higher summer solar insolation at 60°N (10% higher than today), leading to a reduction in sea-ice cover (Sarnthein et al., 2003). As ice cover decreased, additional solar energy was stored in summer and subsequently re-radiated during the winter (e.g. Gildor and Tziperman, 2001). This process accelerated the ice sheet melting, and eventually, its retreat towards the fjord heads (Forwick and Vorren, 2009; Jessen et al., 2010; Baeten et al., 2010). Our data suggest that the iceberg calving to Storfjordrenna was significantly reduced or may have even disappeared at ap-

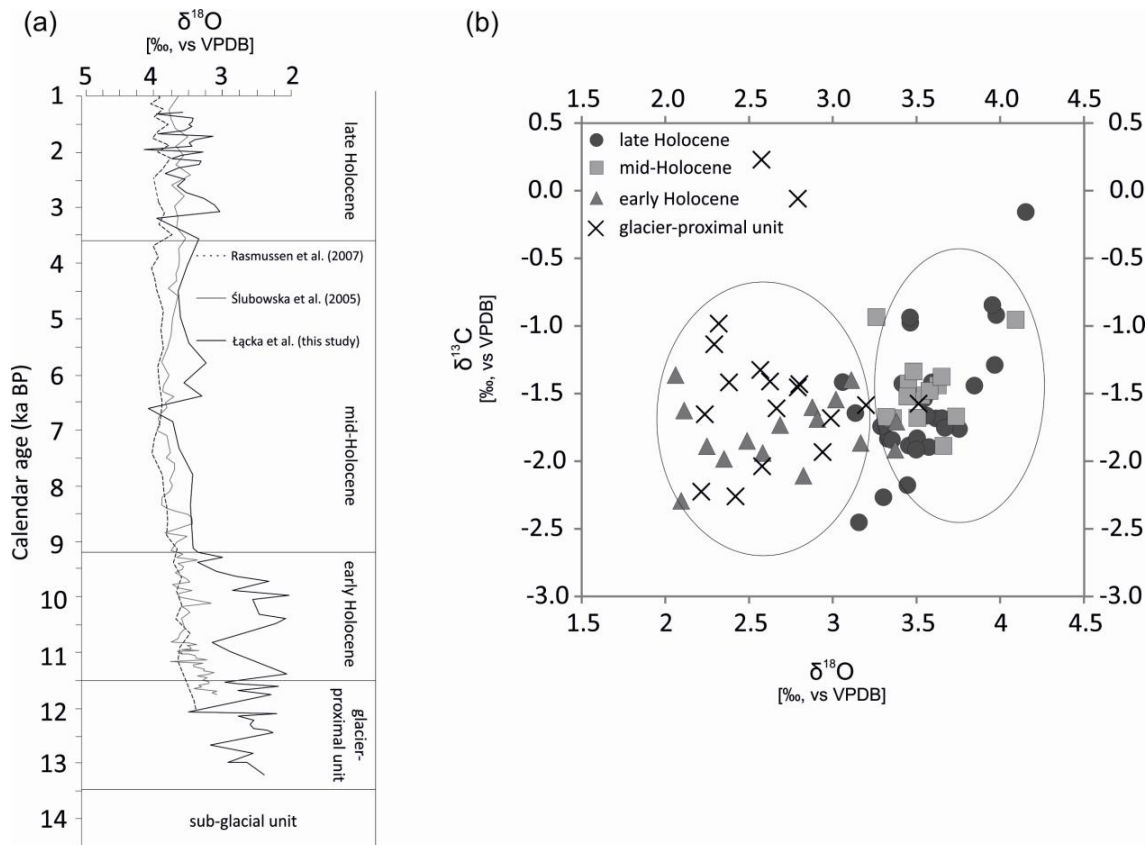


Figure 7. (a) The comparison of $\delta^{18}\text{O}$ records (corrected for ice volume changes) between Łącka et al. (this study; black solid line) and Ślubowska et al. (2005; grey solid line) and Rasmussen et al. (2007; black dashed line) plotted versus thousands of calendar years. The $\delta^{18}\text{O}$ records after Łącka et al. (this study) were measured on *E. excavatum* f. *clavata* and the two latter ones (Ślubowska et al., 2005 and Rasmussen et al., 2007) were measured on *M. barleeanum*. (b) Scatter plot showing $\delta^{13}\text{C}$ versus $\delta^{18}\text{O}$ values from core JM09-020-GC (this study).

proximately 10 800 cal yr BP. However, the supply of turbid meltwater from land to the study area still resulted in a relatively high sediment accumulation rate.

According to Risebrobakken et al. (2011) and Groot et al. (2014), the presence of Arctic Water suppressed the warming signal in the western Barents Sea. This observation is in agreement with our data on planktonic foraminifera reappearing at the termination of the early Holocene (ca. 9600 cal yr BP; Fig. 5). During this period, *N. pachyderma* (sin.) dominated, but certain peaks of *N. pachyderma* (dex.) and *T. quinqueloba* were noted. The two latter species are treated as subpolar species (Bé and Tolderlund, 1971), although *T. quinqueloba* also could be related to oceanic frontal conditions separating Atlantic and Arctic Water (Johannessen et al., 1994; Matthiessen et al., 2001). The peaks of *T. quinqueloba* near 9600 cal yr BP were noted previously in the western Barents Sea margin (e.g. Hald et al., 2007; Risebrobakken et al., 2010).

Increasing foraminiferal biodiversity in Storfjordrenna (Fig. 5) as well as the occurrence of the thermophilous mollusc *Mytilus edulis* on the western Edgeøya (Salvigsen

et al., 1992) suggest that the inflow of AW crossed Storfjordrenna and continued northward to the inner fjord by 9600 cal yr BP.

5.4 Glaciomarine unit II (mid-Holocene; 9200–3600 cal yr BP)

The mid-Holocene was characterised by relatively stable environmental conditions, low sediment accumulation rates ($0.002 \text{ g cm}^{-2} \text{ yr}^{-1}$) and a minor delivery of IRD (Fig. 4), resulting from rather limited ice rafting and a reduced supply of fine-grained material to Storfjordrenna. Low sedimentation rates and the low Fe/Ca ratio reflect the reduced glacial conditions on Svalbard during the mid-Holocene (Elverhøi et al., 1995; Svendsen and Mangerud, 1997). In contrast, Hald et al. (2004) noted that in the record from Van Mijenfjorden, an enhanced tidewater glaciation occurred during this period; it was thus argued that IRD is a more reliable indicator of glaciation than sedimentation rates. However, ice rafting in Storfjordrenna was generally low.

Shifts between the dominant species *C. reniforme* and *E. excavatum* f. *clavata* (Fig. 5) reflect environmental/hydrological changes (Hald and Korsun, 1997). The decrease of *E. excavatum* f. *clavata* (percentage and flux), which prefers colder bottom waters (Sejrup et al., 2004; Sæther et al., 2009) and the increase of *C. reniforme* point to the constant inflow of less modified AW and a reduction in sedimentation (e.g. Schröder-Adams et al., 1990; Bergsten, 1994; Jennings and Helgadóttir, 1994; Hald and Steinsund, 1996; Hald and Korsun, 1997). Furthermore, the relative abundance of *M. barleeanum* (Fig. 5) indicates that environmental conditions in Storfjordrenna were similar to those of contemporary Norwegian fjords that are dominated by AW with a temperature of 6–8 °C and salinities of 34–35 (Husum and Hald, 2004). High total foraminiferal flux at the beginning of this period as well as high foraminiferal species richness and biodiversity clearly point to AW conditions at the bottom (Hald and Korsun, 1997; Majewski and Zajaczkowski, 2007; Włodarska-Kowalczyk et al., 2013). These conclusions are also supported by the heavier $\delta^{18}\text{O}$, which demonstrates AW dominance and a significant reduction in the amount of freshwater and ArW in Storfjordrenna (Fig. 7). The reduced sea-ice condition during the mid-Holocene was also observed on the northern Barents Sea continental margin, seen as an increase in palaeoproductivity (Wollenburg et al., 2004). The continuous presence of *Mytilus edulis* during the entire mid-Holocene points to the reduced inflow of the East Spitsbergen Current due to the AW inflow (Feyling-Hansen, 1955; Forman, 1990; Salvigsen et al., 1992). The pathway and range of AW inflow to the western and northeastern Svalbard during mid-Holocene were well described by Ślubowska-Woldengen et al. (2008) and Groot et al. (2014). Taken together with our results, these observations suggest that one of the main pathways of AW inflow to the eastern Svalbard may have occurred through Storfjordrenna.

Although sediment accumulation rates were low and grain size and geochemical proxies remained relatively constant during the mid-Holocene, the foraminiferal flux (including planktonic foraminifera) increased in two periods of 9000–8000 and 6000–5500 cal yr BP (Figs. 4 and 5, respectively). In both cases, the increase in IRD and *I. norcrossi* fluxes was followed by a slight depletion in $\delta^{18}\text{O}$ and heavier $\delta^{13}\text{C}$, suggesting minor cooling and likely seasonal sea-ice formation leading to beach sediment transport by shore ice. Our observations support earlier studies of the overall mid-Holocene shifts towards a colder environment (Skirbekk et al., 2010; Rasmussen et al., 2012; Berben et al., 2014; Groot et al., 2014; Sternal et al., 2014) and fluctuations in the glacial activity in the Svalbard region (e.g. Forwick and Vorren, 2007, 2009; Beaten et al., 2010; Ojala et al., 2014). Our data show an increased supply of IRD fraction to the Storfjordrenna sediment followed by variation of $\delta^{18}\text{O}$; however, the high flux of *M. barleeanum* associated with Atlantic-derived waters (Steinsund, 1994; Jennings et al., 2006; Fig. 5) indicates an AW condition in southern Storfjorden through-

out the entire mid-Holocene. A similar ameliorated condition with consistent AW inflow also prevailed over the mid-Holocene in the Kveithola Trough south of Storfjordrenna (Berben et al., 2014; Groot et al., 2014). To a lesser extent, these two signals (AW inflow and higher IRD flux) are not necessarily contradictory because snow accumulation on land and inconsiderable glacier advance depend on humid air transport from the ocean. Thus, slight changes in the atmospheric frontal zone over Svalbard could cause fluctuation of the glacier range.

5.5 Glaciomarine unit III (late Holocene; 3600–1200 cal yr BP)

The late Holocene is characterised by a gradual increase in sediment accumulation rates followed by numerous sharp peaks of sand content and minor peaks of IRD flux as well as an increased Fe/Ca ratio, thus indicating ice growth on land (compare with e.g. Svendsen and Mangerud, 1997; Hald et al., 2004; Forwick and Vorren, 2009; Taldenkova et al., 2012; Kempf et al., 2013) and slightly enhanced iceberg calving and/or ice rafting over the core site. The IRD record shows few irregular small peaks in the late Holocene (Fig. 6), which could be correlated with enhanced sea currents that increase the drift of the icebergs, according to Hass (2002). Forwick et al. (2010) suggested several glacier front fluctuations during the past two millennia in Sassenfjorden and Tempelfjorden (W Spitsbergen), and hence we assume that increased iceberg calving occurred at Storfjordrenna during this time. However, increased IRD flux can also reflect deposition related to enhanced shore ice rafting. The latter explanation is in agreement with the heavier $\delta^{18}\text{O}$ record (Fig. 5), indicating a minor cooling.

The mean grain size ($> 63\ \mu\text{m}$) increases in the late Holocene (Fig. 4) and may indicate stronger bottom current velocities and winnowing of fine-grained sediments. Andrúleit et al. (1996) observed similar increased erosive activity of bottom currents during the late Holocene on the SW Svalbard shelf. This sudden increase in current velocities might be connected with (1) postglacial reorganisation of oceanographic conditions, (2) relative lowering of the sea level during the postglacial isostatic rebound and/or (3) more intensive sea-ice formation that enhanced the formation of BSW, thus forming a seasonal near-bottom dense water mass flowing over the coring site (Andrúleit et al., 1996). Nevertheless, this process is still not fully understood.

The sharp increase in the foraminiferal flux (Fig. 4) pointing to the increased nutrient advection/upwelling and biological productivity at the coring site during the late Holocene was likely caused by variable hydrological conditions and most likely strong gradients leading to the formation of hydrological fronts. In contrast, Wollenburg et al. (2004) noted reduced palaeoproductivity in the northern Barents Sea over the entire late Holocene, pointing to several events of heavy sea-ice cover. Our data show increased fluxes of opportunis-

tic species *E. excavatum* and *C. reniforme* as well as an abundance of *N. labradorica* and *Islandiella* spp. *N. labradorica* and *Islandiella* spp. in areas with a high biological productivity in the upper surface waters (e.g. Hald and Steinsund, 1996; Korsun and Hald, 2000; Knudsen et al., 2012). Abundant though variable *M. barleeianum* is documented in organic-rich mud within troughs of the Barents Sea (Hald and Steinsund, 1996) and in temperate fjords of Norway (Husum and Hald, 2004), which points to high productivity in the euphotic zone leading to enhanced export of organic material/nutrients to the sea floor. Our data also show high *N. pachyderma* flux throughout this unit, reflecting a significant increase of euphotic productivity at the coring site. However, a low percentage of dextral specimens and *T. quinqueloba* point to low sea-surface temperatures (Fig. 5). This observation is in agreement with Rasmussen et al. (2014), who noted that after ca. 3700 cal yr BP, Atlantic Water was only sporadically present at the surface. Cooling at the sea surface reflects the general trend in the Northern Hemisphere related to orbital forcing and reduction of summer insolation at high latitudes over the late Holocene (Wanner et al., 2008).

The last evidence of AW inflow to Edgøya area based on *M. edulis* is dated to 5000 cal yr BP (Hjort et al., 1995). After that time, *M. edulis* remained absent until the present time; however, its disappearance could be related to the freshening of Surface Water (Berge et al., 2006) and sea-ice forcing as opposed to the extinction of AW in Storfjorden over the late Holocene (Rasmussen et al., 2007).

6 Conclusions

Multi-proxy analyses of one sediment core provide new information on the environmental development of the central portion of Storfjordrenna off the southern Svalbard since the late Bølling–Allerød. The main conclusions of our study are described as follows:

- Central Storfjordrenna was deglaciated prior to ~13 950 cal yr BP, and these new data may aid in refining future models of Svalbard–Barents Ice Sheet deglaciation.
- Between ca. 13 450 and 11 500 cal yr BP, Storfjordrenna remained under the influence of Arctic Water masses with sea-ice cover episodically limiting the drift of icebergs. Nevertheless, at least three peaks in temperature that occurred during the Younger Dryas stadial (12 800–11 500 cal yr BP) presumably led to the seasonal disappearance of sea-ice and significantly enhanced IRD flux, thus indicating more sub-polar conditions.
- Atlantic Water began to flow onto the shelves off Svalbard and into Storfjorden during the early Holocene, leading to progressive warming and significant glacial melting. From ca. 9600 cal yr BP, Atlantic Water dominated the water column in Storfjordrenna.

- The environmental conditions off eastern Svalbard remained relatively stable from 9200 to 3600 cal yr BP, with glaciers smaller than those of today. However, certain small-scale cooling events (9000–8000 and 6000–5500 cal yr BP) indicate minor fluctuations in the climate/oceanography of Storfjordrenna.
- A surface-water cooling and freshening occurred in Storfjordrenna during the late Holocene, synchronous with glacier growth and cooling on land and the presence of AW in the deeper portion of Storfjordrenna. The late Holocene in Storfjordrenna experienced increased bottom current velocities; however, the driving mechanism is not fully understood.

Acknowledgements. The study was supported by the Institute of Oceanology Polish Academy of Science and the Polish Ministry of Science and Higher Education with grant no. NN 306 469938. The ¹⁴C dating was funded by the Polish Ministry of Science and Higher Education grant no. IP2010 040970. We thank the captain and crew of R/V *Jan Mayen*, as well as the cruise participants, in particular Steinar Iversen, for their help at sea. Trine Dahl and Ingvild Hald are acknowledged for the acquisition of X-radiographs. Tine Rasmussen (UiT) is gratefully acknowledged for sharing the data with us. Katarzyna Zamelczyk (UiT) and Maria Włodarska-Kowalczyk (IOPAS) are thanked for help in planktonic foraminifera (Katarzyna) and bivalves (Maria) determination. Patrycja Jernas (UiT) helped during subsampling of the cores. Master's students from the University of Gdansk Kamila Sobala and Anna Nowicka helped with the Mastersizer 2000 analysis. We are very grateful to Renata Lucchi (Istituto Nazionale di Oceanografia e Geofisica Sperimentale, Italy), Reignheid Skogseth (University Centre in Svalbard) and Ilona Goszczko (IOPAS) for the comments on the early version of this paper. We are sincerely indebted to Amy Lusher (Galway-Mayo Institute of Technology), Sara Strey-Mellema (University of Illinois) and Christof Pearce (Stockholm University) for improving the English of this manuscript. The comments from Thomas Cronin and an anonymous reviewer helped to improve the paper considerably.

Edited by: D.-D. Rousseau

References

- Aagaard, K., Foldvik, A., and Hillman, S.: The West Spitsbergen Current: disposition and water mass transformation, *J. Geophys. Res.*, 92, 3778–3784, 1987.
- Akimova, A., Schauer, U., Danilov, S., and Núñez-Riboni, I.: The role of the deep mixing in the Storfjorden shelf water plume, *Deep-Sea Res. Pt. I*, 58, 403–414, 2011.
- Alley, R.: The younger Dryas cold interval as viewed from central Greenland, *Quaternary Sci. Rev.*, 19, 213–226, 2000.
- Alve, E. and Goldstein, S. T.: Dispersal, survival and delayed growth of benthic foraminiferal propagules, *J. Sea Res.*, 63, 36–51, 2010.

- Andreassen, K., Winsborrow, M., Bjarnadóttir, L. R., and Rütther, D. C.: Ice stream retreat dynamics inferred from an assemblage of landforms in the northern Barents Sea, *Quaternary Sci. Rev.*, 92, 246–257, doi:10.1016/j.quascirev.2013.09.015, 2014.
- Andrulleit, H., Freiwald, A., and Schäfer, P.: Bioclastic carbonate sediments on the southwestern Svalbard shelf, *Mar. Geol.*, 134, 163–182, 1996.
- Baeten, N. J., Forwick, M., Vogt, C., and Vorren, T. O.: Late Weichselian and Holocene sedimentary environments and glacial activity in Billefjorden, Svalbard, in: *Fjord Systems and Archives*, edited by: Howe, J. A., Austin, W. E. N., Forwick, M., and Paetzel, M., Geological Society, London, Special Publications, 344, 207–223, 2010.
- Bakke, J., Lie, Ø., Heegaard, E., Dokken, T., Haug, G. H., Birks, H. H., Dulski, P., and Nilsen, T.: Rapid oceanic and atmospheric changes during the Younger Dryas cold period, *Nat. Geosci.*, 2, 202–205, 2009.
- Bauch, H. A., Erlenkeuser, H., Bauch, D., Mueller-Lupp, T., and Taldenkova, E.: Stable oxygen and carbon isotopes in modern benthic foraminifera from the Laptev Sea shelf: implications for reconstruction proglacial and profluvial environments in the Arctic, *Mar. Micropaleontol.*, 51, 285–300, 2004.
- Bé, A. W. H. and Tolderlund, D. S.: Distribution and ecology of living planktonic foraminifera in surface waters of the Atlantic and Indian oceans, in: *The Micropaleontology of Oceans*, edited by: Funnell, B. M. and Riedel, W. R., Cambridge University Press, Cambridge, UK, 105–149, 1971.
- Berben, S. M. P., Husum, K., Cabedo-Sanz, P., and Belt, S. T.: Holocene sub-centennial evolution of Atlantic water inflow and sea ice distribution in the western Barents Sea, *Clim. Past*, 10, 181–198, doi:10.5194/cp-10-181-2014, 2014.
- Berge, J., Johnsen, G., Nilsen, F., Gulliksen, B., Slagstad, D., and Pampanin, D. M.: The *Mytilus edulis* population in Svalbard: how and why, *Mar. Ecol.-Prog. Ser.*, 309, 305–306, 2006.
- Bergsten, H.: Recent benthic foraminifera of a transect from the North Pole to the Yermak Plateau, eastern central Arctic Ocean, *Mar. Geol.*, 119, 251–267, 1994.
- Blott, S. J. and Pye, K.: GRADISTAT: a grain size distribution and statistics package for the analysis of unconsolidated sediments, *Earth Surf. Proc. Land.*, 26, 1237–1248, 2001.
- Broecker, W. S.: Was the younger Dryas triggered by a flood?, *Science*, 312, 1146–1148, doi:10.1126/science.1123253, 2006.
- Cronin, T. M., Rayburn, J. A., Guilbault, J.-P., Thunell, R., and Franzi, D. A.: Stable isotope evidence for glacial lake drainage through the St. Lawrence Estuary, eastern Canada, ~13.1–12.9 ka, *Quaternary Sci. Rev.*, 260, 55–65, 2012.
- Croudace, I. W., Rindby, A., and Rothwell, R. G.: ITRAX: description and evaluation of a new multi-function X-ray core scanner, Geological Society, London, Special Publications, 267, 51–63, 2006.
- Czernik, J. and Goslar, T.: Preparation of graphite targets in the Gliwice Radiocarbon Laboratory for AMS ¹⁴C dating, *Radiocarbon*, 43, 283–291, 2001.
- Dansgaard, W., Johnsen, S. J., Clausen, H. B., Dahl-Jensen, D., Gundestrup, N. S., Hammer, C. U. C., Hvidberg, S., Steffensen, J. P., Sveinbjörnsdóttir, A. E., Jouzel, J., and Bond, G.: Evidence for general instability of past climate from a 250-kyr ice-core record, *Nature*, 364, 218–220, doi:10.1038/364218a0, 1993.
- Dowdeswell, J. A., Elverhøi, A., and Spielhagen, R.: Glacimarine sedimentary processes and facies on the polar north Atlantic margins, *Quaternary Sci. Rev.*, 17, 243–272, 1998.
- Duplessy, J. C., Cortijo, E., Ivanova, E., Khusid, T., Labeyrie, L., Levitan, M., Murdmaa, I., and Paterne, M.: Paleooceanography of the Barents Sea during the Holocene, *Paleoceanography*, 20, PA4004, doi:10.1029/2004PA001116, 2005.
- Dylmer, C. V., Giraudeau, J., Eynaud, F., Husum, K., and De Vernal, A.: Northward advection of Atlantic water in the eastern Nordic Seas over the last 3000 yr, *Clim. Past*, 9, 1505–1518, doi:10.5194/cp-9-1505-2013, 2013.
- Eldevik, T., Risebrobakken, B., Bjune, A. E., Andersson, C., Birks, H. J. B., Dokken, T. M., Drange, H., Glessmer, M. S., Li, C., Nilsen, J. E. Ø., Otterå, O. H., Richter, H., and Skagseth, Ø.: A brief history of climate – the northern seas from the Last Glacial Maximum to global warming, *Quaternary Sci. Rev.*, 106, 225–246, 2014.
- Elmore, A. C. and Wright, J. D.: North Atlantic Deep Water and climate variability during the younger Dryas cold period, *Geology*, 39, 107–110, 2011.
- Elverhøi, A., Svendsen, J. I., Solheim, A., Andersen, E. S., Milliman, J., Mangerud, J., and Hooke, R. L.: Late quaternary sediment yield from the high Arctic Svalbard area, *J. Geol.*, 103, 1–17, 1995.
- Fer, I., Skogseth, R., Haugan, P. M., and Jaccard, P.: Observations of the Storfjorden overflow, *Deep-Sea Res. Pt. I*, 50, 1283–1303, doi:10.1016/S0967-0637(03)00124-9, 2003.
- Fer, I., Skogseth, R., and Haugan, P. M.: Mixing of the Storfjorden overflow (Svalbard Archipelago) inferred from density overturns, *J. Geophys. Res.*, 109, C01005, doi:10.1029/2003JC001968, 2004.
- Feyling-Hanssen, R.: Stratigraphy of the marine late-Pleistocene of Billefjorden, Vestspitsbergen, *Norsk Polarinst. Skri.*, 107, 1–186, 1955.
- Feyling-Hanssen, R. and Jørstad, F.: Quaternary fossil from the Sassen-area in Isfjorden, west-Spitsbergen (the marine mollusk fauna), *Norsk Polarinst. Skri.*, 94, 1–85, 1950.
- Forman, S. L.: Post-glacial relative sea level history of northwestern Spitsbergen, Svalbard, *Bull. Geol. Soc. Am.*, 102, 1580–1590, 1990.
- Forman, S. L., Lubinski, D. J., Ingólfsson, Ó., Zeeberg, J. J., Snyder, J. A., Siegert, M. J., and Matishov, G. G.: A review of postglacial emergence on Svalbard, Franz Josef Land and Novaya Zemlya, northern Eurasia, *Quaternary Sci. Rev.*, 23, 1391–1434, 2004.
- Forwick, M. and Vorren, T. O.: Holocene mass-transport activity in and climate outer Isfjorden, Spitsbergen: marine and subsurface evidence, *Holocene*, 17, 707–716, 2007.
- Forwick, M. and Vorren, T. O.: Late Weichselian and Holocene sedimentary environments and ice rafting in Isfjorden, Spitsbergen, *Palaeogeogr. Palaeoclimatol.*, 280, 258–274, 2009.
- Forwick, M., Vorren, T. O., Hald, M., Korsun, S., Roh, Y., Vogt, C., and Yoo, K.-C.: Spatial and temporal influence of glaciers and rivers on the sedimentary environment in Sassenfjorden and Tempelfjorden, Spitsbergen, in: *Fjord Systems and Archives*, edited by: Howe, J. A., Austin, W. E. N., Forwick, M., and Paetzel, M., Geological Society, London, Special Publications, 344, 163–193, 2010.
- Gammelsrod, T. and Rudels, B.: Hydrographic and current measurements in the Fram Strait, *Pol. Res.*, 1, 115–126, 1983.

- Geyer, F., Fer, I., and Smedsrud, L. H.: Structure and forcing of the overflow at the Storfjorden sill and its connection to the Arctic coastal polynya in Storfjorden, *Ocean Sci.*, 6, 401–411, doi:10.5194/os-6-401-2010, 2010.
- Gilbert, R.: Environmental assessment from the sedimentary record of highlatitude fiords, *Geomorphology*, 32, 295–314, 2000.
- Gildor, H. and Tziperman, E.: A sea ice climate switch mechanism for the 100 kyr glacial cycles, *J. Geophys. Res.*, 106, 9117–9133, 2001.
- Goslar, T., Czernik, J., and Goslar, E.: Low-energy ^{14}C AMS in Poznań Radiocarbon Laboratory, Poland, *Nucl. Instrum. Meth. B*, 223/224, 5–11, 2004.
- Groot, D. E., Aagaard-Sørensen, S., and Husum, K.: Reconstruction of Atlantic water variability during the Holocene in the western Barents Sea, *Clim. Past*, 10, 51–62, doi:10.5194/cp-10-51-2014, 2014.
- Grootes, P. M., Stuiver, M., White, J. W. C., Johnsen, S. J., and Jouzel, J.: Comparison of oxygen isotope records from the GISP2 and GRIP Greenland ice cores, *Nature*, 366, 552–554, 1993.
- Haarpaintner, J., Gascard, J., and Haugan, P. M.: Ice production and brine formation in Storfjorden, Svalbard, *J. Geophys. Res.*, 106, 14001–140013, doi:10.1029/1999JC000133, 2001.
- Hald, M. and Korsun, S.: Distribution of modern Arctic benthic foraminifera from fjords of Svalbard, *J. Foramin. Res.*, 27, 101–122, 1997.
- Hald, M. and Steinsund, P. I.: Benthic foraminifera and carbonate dissolution in surface sediments of the Barents- and Kara Seas, Surface-sediment composition and sedimentary processes in the central Arctic Ocean and along the Eurasian Continental Margin, *Ber. Polarforsch.*, 212, 285–307, 1996.
- Hald, M., Ebbesen, H., Forwick, M., Godtlielsen, F., Khomenko, L., Korsun, S., Olsen, L. R., and Vorren, T. O.: Holocene paleoceanography and glacial history of the West Spitsbergen area, Euro-Arctic margin, *Quaternary Sci. Rev.*, 23, 2075–2088, 2004.
- Hald, M., Andersson, C., Ebbesen, H., Jansen, E., Klitgaard-Kristensen, D., Risebrobakken, B., Salomonsen, G. R., Sarnthein, M., Sejrup, H. P., and Telford, R. J.: Variations in temperature and extent of Atlantic Water in the Northern North Atlantic during the Holocene, *Quaternary Sci. Rev.*, 26, 3423–40, 2007.
- Hansen, J., Hanken, N.-M., Nielsen, J. K., Nielsen, J. K., and Thomsen, E.: Late Pleistocene and Holocene distribution of *Mytilus edulis* in the Barents Sea region and its paleoclimatic implications, *J. Biogeogr.*, 38, 1197–1212, 2011.
- Hass, H. C.: A method to reduce the influence of ice-rafted debris on a grain size record from northern Fram Strait, *Polar Res.*, 21, 299–306, 2002.
- Hjort, C., Andrielson, L., Bondevik, S., Landvik, J., Mangerud, J., and Salvigsen, O.: *Mytilus edulis* on eastern Svalbard – dating the Holocene Atlantic Water influx maximum, in: Weichselian and Holocene glacial and marine history of East Svalbard: preliminary report on the PONAM field work in 1991, edited by: Moller, P., Hjort, C., and Ingolfsson, O., *Lundqua Rep.*, 35, 171–175, 1992.
- Hjort, C., Mangerud, J., Andrielson, L., Bondevik, S., Landvik, J. Y., and Salvigsen, O.: Radiocarbon dated common mussels *Mytilus edulis* from eastern Svalbard and the Holocene marine climatic optimum, *Polar Res.*, 14, 239–243, 1995.
- Hormes, A., Gjermundsen, E. F., and Rasmussen, T. L.: From mountain top to the deep sea – deglaciation in 4-D of the north-western Barents Sea, *Quaternary Sci. Rev.*, 75, 78–99, 2013.
- Husum, K. and Hald, M.: A continuous marine record 8000–1600 cal yr BP from the Malangenfjord, north Norway: foraminiferal and isotopic evidence, *Holocene*, 14, 877–887, 2004.
- Jennings, A. E. and Helgadottir, G.: Foraminiferal assemblages from the fjords and shelf of Eastern Greenland, *J. Foramin. Res.*, 24, 123–44, 1994.
- Jennings, A. E., Hald, M., Smith, M., and Andrews, J. T.: Fresh-water forcing from the Greenland Ice Sheet during the Younger Dryas: evidence from southeastern Greenland shelf cores, *Quaternary Sci. Rev.*, 25, 282–298, 2006.
- Jessen, S. P., Rasmussen, T. L., Nielsen, T., and Solheim, A.: A new late Weichselian and Holocene marine chronology for the western Svalbard slope 30 000–0 Cal years BP, *Quaternary Sci. Rev.*, 29, 1301–1312, doi:10.1016/j.quascirev.2010.02.020, 2010.
- Johannessen, T., Jansen, E., Flatøy, A., and Ravelo, A. C.: The relationship between surface water masses, oceanographic fronts and paleoclimatic proxies in surface sediments of the Greenland, Iceland, Norwegian Seas, in: Carbon cycling in glacial ocean: constraints on the ocean's role in global change, edited by: Zahn, R., Kominski, M., and Labyrie, L., Springer-Verlag, 61–85, 1994.
- Kaufman, D. S., Ager, T. A., Anderson, N. J., Anderson, P. M., Andrews, J. T., Bartlein, P. J., Brubaker, L. B., Coats, L. L., Cwynar, L. C., Duvall, M. L., Dyke, A. S., Edwards, M. E., Eisner, W. R., Gajewski, K., Geirsdóttir, A., Hu, F. S., Jennings, A. E., Kaplan, M. R., Kerwin, M. W., Lozhkin, A. V., MacDonald, G. M., Miller, G. H., Mock, C. J., Oswald, W. W., Otto-Bliesner, B. L., Porinchu, D. F., Rühland, K., Smol, J. P., Steig, E. J., and Wolfe, B. B.: Holocene thermal maximum in the western Arctic (0–180° W), *Quaternary Sci. Rev.*, 23, 529–560, 2004.
- Kempf, P., Forwick, M., Laberg, J. S., and Vorren, T. O.: Late Weichselian – Holocene sedimentary palaeoenvironment and glacial activity in the high-Arctic van Keulenfjorden, Spitsbergen, *Holocene*, 23, 1605–1616, 2013.
- Klitgaard Kristensen, D., Rasmussen, T. L., and Koç, N.: Palaeoceanographic changes in the northern Barents Sea during the last 16 000 years – new constraints on the last deglaciation of the Svalbard-Barents Sea Ice Sheet, *Boreas*, 42, 798–813, 2013.
- Knudsen, K. L., Eiríksson, J., and Bartels-Jónsdóttir, H. B.: Oceanographic changes through the last millennium off North Iceland: temperature and salinity reconstructions based on foraminifera and stable isotopes, *Mar. Micropaleontol.*, 54–73, 2012.
- Korsun, S. and Hald, M.: Modern benthic foraminifera off tide water glaciers, Novaja Semlja, Russian Arctic, *Arctic Alpine Res.*, 30, 61–77, 1998.
- Korsun, S. and Hald, M.: Seasonal dynamics of benthic foraminifera in a glacially fed fjord of Svalbard, *European Arctic, J. Foramin. Res.*, 30, 251–271, 2000.
- Kubischta, F., Knudsen, K. L., Kaakinen, A., and Salonen, V.-P.: Late Quaternary foraminiferal record in Murchisonfjorden, Nordaustlandet, Svalbard, *Polar Res.*, 29, 283–297, 2010.
- Łącka, M., Zajączkowski, M., Pawłowska, J., Forwick, M., and Szczuciński, M.: The 600-years record of Atlantic Water variability in the Storfjordrenna, in preparation, 2015.

- Landvik, J. Y., Hjort, C., Mangerud, J., Möller, P., and Salvigsen, O.: The Quaternary record of eastern Svalbard: an overview, *Polar Res.*, 14, 95–103, 1995.
- Loeblich, A. R. and Tappan, H.: *Foraminiferal Genera and Their Classification*, Van Nostrand Reinhold, New York, 970 pp., 1987.
- Loeng, H.: Features of the physical oceanographic conditions of the Barents Sea, *Polar Res.*, 10, 5–18, 1991.
- Lucchi, R. G., Camerlenghi, A., Rebesco, M., Colmenero-Hidalgo, E., Sierro, F. J., Sagnotti, L., Urgeles, R., Melis, R., Morigi, C., Bárcena, M.-A., Giorgetti, G., Villa, G., Persico, D., Flores, J.-A., Rigual-Hernández, A. S., Pedrosa, M. T., Macri, P., and Caburlotto, A.: Postglacial sedimentary processes on the Storfjorden and Kveithola trough mouth fans: Significance of extreme glacial sedimentation, *Global Planet. Change*, 111, 309–326, 2013.
- Lydersen, C., Nøst, O., Lovell, P., McConell, B., Gammelsrød, T., Hunter, C., Fedak, M., and Kovacs, K.: Salinity and temperature structure of a freezing Arctic fjord – monitored by white whales (*Delphinapterus leucas*), *Geophys. Res. Lett.*, 29, 2119, doi:10.1029/2002GL015462, 2002.
- Majewski, W. and Zajaczkowski, M.: Benthic foraminifera in Adventfjorden, Svalbard: Last 50 years of local hydrographic changes, *J. Foramin. Res.*, 37, 107–124, 2007.
- Mangerud, J., Bondevik, S., Gulliksen, S., Hufthammer, A. K., and Høisæter, T.: Marine ^{14}C reservoir ages for 19th century whales and molluscs from the North Atlantic, *Quaternary Sci. Rev.*, 25, 3228–3245, 2006.
- Matthiessen, J., Baumann, K. H., Schröder-Ritzrau, A., Hass, C., Andrulleit, H., Baumann, A., Jensen, S., Kohly, A., Pflaumann, U., Samtleben, C., Schäfer, P., and Thiede, J.: Distribution of calcareous, siliceous and organic-walled planktic microfossils in surface sediments of the Nordic seas and their relation to surface-water masses, in: *The northern North Atlantic: a changing environment*, edited by: Schäfer, P., Ritzrau, W., Schlüter, M., and Thiede, J., Springer, 105–27, 2001.
- Mayewski, P. A., Meeker, L. D., Morrison, M. C., Twickler, M. S., Whitlow, S. I., Ferland, K. K., Meese, D. A., Legrand, M. R., and Steffensen, J. P.: Greenland ice core “signal” characteristics: an expanded view of climate change, *J. Geophys. Res.*, 98, 12839–12847, doi:10.1029/93JD01085, 1993.
- Munsell® *Color Geological Rock: Color Chart Revised Washable Edition*, Geological Society of America (GSA), 2009.
- Murton, J. B., Bateman, M. D., Dallimore, S. R., Teller, J. T., and Yang, Z.: Identification of Younger Dryas outburst flood path from Lake Agassiz to the Arctic Ocean, *Nature*, 464, 740–743, 2010.
- Norges Sjøkartverk: *Den norske los – Arctic pilot*, Farvannbeskrivelse, sailing directions, Svalbard–Jan Mayen, 7th Edn., Stavanger, Norwegian Hydrographic Service, Norwegian Polar Institute, Tromsø, 1988.
- O’Dwyer, J., Kasajima, Y., and Nøst, O.: North Atlantic water in the Barents Sea opening, 1997 to 1999, *Polar Res.*, 2, 209–216, 2001.
- Ojala, A. E. K., Salonen, V.-P., Moskalik, M., Kubischta, F., and Oinonen, M.: Holocene sedimentary environment of a High-Arctic fjord in Nordaustlandet, Svalbard, *Pol. Polar Res.*, 35, 73–98, 2014.
- Østby, K. L. and Nagy, J.: Foraminiferal distribution in the Western Barents Sea, recent and quaternary, *Polar Res.*, 1, 55–95, 1982.
- Osterman, L. E. and Nelson, A. R.: Latest Quaternary and Holocene paleoceanography of the eastern Baffin Island continental shelf, Canada: benthic foraminiferal evidence, *Can. J. Earth Sci.*, 26, 2236–2248, 1989.
- Ottesen, D., Dowdeswel, L. J. A., and Rise, L.: Submarine landforms and the reconstruction of fast-flowing ice streams within a large Quaternary ice sheet: the 2500 km-long Norwegian–Svalbard margin (57–80° N), *Geol. Soc. Am. Bull.*, 117, 1033–1050, 2005.
- Pearce, C., Seidenkrantz, M.-S., Kuijpers, A., Massé, G., Reynisson, N. F., and Kristiansen, S. M.: Ocean lead at the termination of the Younger Dryas cold spell, *Nature Communications*, 4, 1664, doi:10.1038/ncomms2686, 2013.
- Pedrosa, M. T., Camerlenghi, A., de Mol, B., Urgeles, R., Rebesco, M., Lucchi, R. G., Amblas, D., Calafat, A., Canals, M., Casamor, J. L., Costa, S., Frigola, J., Iglesias, O., Lafuerza, S., Lastras, G., Lavoie, C., Liquete, C., Hidalgo, E. C., Flores, J. A., Sierro, F. J., Carburlo, A., Grossi, M., Winsborrow, M., Zgur, F., Deponte, D., De Vittor, C., Facchin, L., Tomini, I., De Vittor, R., Pelos, C., Persissinotto, G., Ferrante, N., and Di Curzio, E.: Seabed morphology and shallow sedimentary structure of the Storfjorden and Kveithola trough-mouth fans northwest Barents Sea, *Mar. Geol.*, 286, 1–4, 2011.
- Piechura, J.: Dense bottom waters in Storfjord and Storfjordrenna, *Oceanologia*, 38, 285–292, 1996.
- Polyak, L. and Mikhailov, V.: Post-glacial environments of the southeastern Barents Sea: Foraminiferal evidence, *Geological Society, London, Special Publications*, 111, 323–337, 1996.
- Polyak, L. and Solheim, A.: Late- and post-glacial environments in the northern Barents Sea west of Franz Josef Land, *Polar Res.*, 13, 97–207, 1994.
- Quadfasel, D., Rudels, B., and Kurz, K.: Outflow of dense water from a Svalbard fjord into the Fram Strait, *Deep-Sea Res.*, 35, 1143–1150, 1988.
- Quadfasel, D. A., Sy, A., Wells, D., and Tunik, A.: Warming in the Arctic, *Nature*, 350, 6317, doi:10.1038/350385a0, 1991.
- Rasmussen, T. L. and Thomsen, E.: Stable isotope signals from brines in the Barents Sea: implications for brine formation during the last glaciation, *Geology*, 37, 903–906, doi:10.1130/G25543A.1, 2009.
- Rasmussen, T. L. and Thomsen, E.: Brine formation in relation to climate changes and ice retreat during the last 15,000 years in Storfjorden, Svalbard, 76–78° N, *Paleoceanography*, 29, 911–929, doi:10.1002/2014PA002643, 2014.
- Rasmussen, T. L. and Thomsen, E.: Palaeoceanographic development in Storfjorden, Svalbard, during the deglaciation and Holocene: evidence from benthic foraminiferal records, *Boreas*, 44, 24–44, doi:10.1111/bor.12098, 2015.
- Rasmussen, T. L., Thomsen, E., Slubowska-Woldengen, M., Jessen, S., Solheim, A., and Koc, N.: Paleoceanographic evolution of the SW Svalbard margin (76° N) since 20 000 ^{14}C yr BP, *Quaternary Res.*, 67, 100–114, doi:10.1016/j.yqres.2006.07.002, 2007.
- Rasmussen, T. L., Forwick, M., and Mackensen, A.: Reconstruction of inflow of Atlantic Water to Isfjorden, Svalbard during the Holocene: correlation to climate and seasonality, *Mar. Micropaleontol.*, 94–95, 80–90, doi:10.1016/j.marmicro.2012.06.008, 2012.
- Rasmussen, T. L., Thomsen, E., Skirbekk, K., Ślubowska-Woldengen, M., Klitgaard Kristensen, D., and Koç, N.: Spa-

- tial and temporal distribution of Holocene temperature maxima in the northern Nordic seas: interplay of Atlantic-, Arctic- and polar water masses, *Quaternary Sci. Rev.*, 92, 280–291, doi:10.1016/j.quascirev.2013.10.034, 2013.
- Rasmussen, T. L., Thomsen, E., Skirbekk, K., Ślubowska-Woldengen, M., Klitgaard Kristensen, D., and Koç, N.: Spatial and temporal distribution of Holocene temperature maxima in the northern Nordic seas: interplay of Atlantic-, Arctic- and polar water masses, *Quaternary Sci. Rev.*, 92, 280–291, doi:10.1016/j.quascirev.2013.10.034, 2014.
- Reimer, P. J., Bard, E., Bayliss, A., Beck, J. W., Blackwell, P. G., Bronk Ramsey, C., Buck, C. E., Cheng, H., Edwards, R. L., Friedrich, M., Grootes, P. M., Guilderson, T. P., Haffidason, H., Hajdas, I., HattĀŚ, C., Heaton, T. J., Hogg, A. G., Hughen, K. A., Kaiser, K. F., Kromer, B., Manning, S. W., Niu, M., Reimer, R. W., Richards, D. A., Scott, E. M., Southon, J. R., Turney, C. S. M., and van der Plicht, J.: IntCal13 and MARINE13 radiocarbon age calibration curves 0–50,000 years cal BP, *Radio-carbon*, 55, 1869–1887, 2013.
- Risebrobakken, B., Moros, M., Ivanova, E. V., Chistyakova, N., and Rosenberg, R.: Climate and oceanographic variability in the SW Barents Sea during the Holocene, *The Holocene*, 20, 609–621, doi:10.1177/0959683609356586, 2010.
- Risebrobakken, B., Dokken, T., Smedsrud, L., Andersson, C., Jansen, E., Moros, M., and Ivanova, E.: Early Holocene temperature variability in the Nordic Seas: The role of oceanic heat advection versus changes in orbital forcing, *Paleoceanography*, 26, PA4206, doi:10.1029/2011PA002117, 2011.
- Rüther, D., Bjarnadóttir, L., R., Junntila, J., Husum, K., Rasmussen, T. L., Lucchi, R. G., and Andreassen, K.: Pattern and timing of the northwestern Barents Sea Ice Sheet deglaciation and indications of episodic Holocene deposition, *Boreas*, 41, 494–512, doi:10.1111/j.1502-3885.2011.00244.x, 2012.
- Saher, M. H., Klitgaard Kristensen, D., Hald, M., Korsun, S., and Jørgensen, L. L.: Benthic foraminifera assemblages in the Central Barents Sea: an evaluation of the effect of combining live and total fauna studies in tracking environmental change, *Norw. J. Geol.*, 89, 149–161, 2009.
- Salvigsen, O., Forman, S., and Miller, G.: Thermophilous mollusks on Svalbard during the Holocene and their paleoclimatic implications, *Polar Res.*, 11, 1–10, 1992.
- Sarnthein, M., van Kreveland, S., Erlenkeuser, H., Grootes, P. M., Kucera, M., Pflaumann, U., and Sculz, M.: Centennial-to-millennial-scale periodicities of Holocene climate and sediment injections off the western Barents shelf, 75° N, *Boreas*, 32, 447–461, 2003.
- Schauer, U.: The release of brine-enriched shelf water from Storfjord into the Norwegian Sea, *J. Geophys. Res.*, 100, 60515–16028, 1995.
- Schauer, U. and Fahrbach, E.: A dense bottom water plume in the western Barents Sea: downstream modification and interannual variability, *Deep-Sea Res. Pt. I*, 46, 2095–2108, 1999.
- Schauer, U., Fahrbach, E., Østerhus, S., and Rohardt, G.: Arctic Warming through the Fram Strait: oceanic heat transport from 3 years of measurements, *J. Geophys. Res.*, 109, C06026, doi:10.1029/2003JC001823, 2004.
- Schröder-Adams, C. J., Cole, F. E., Medioli, F. S., Mudie, P. J., Scott, D. B., and Dobbin, L.: Recent Arctic shelf foraminifera: seasonally ice covered areas vs. perennially ice covered areas, *J. Foramin. Res.*, 20, 8–36, 1990.
- Sejrup, H. P., Birks, H. J. B., Kristensen, D. K., and Madsen, H.: Benthonic foraminiferal distributions and quantitative transfer functions for the northwest European continental margin, *Mar. Micropaleontology*, 53, 197–226, doi:10.1016/j.marmicro.2004.05.009, 2004.
- Serreze, M. C., Maslanik, J. A., Scambos, T. A., Fetterer, F., Stroeve, J., Knowles, K., Fowler, C., Drobot, S., Barry, R. G., and Haran, T. M.: A new record minimum Arctic sea ice and extent in 2002, *Geophys. Res. Lett.*, 30, 1110, doi:10.1029/2002GL016406, 2003.
- Siegert, M. J. and Dowdeswell, J. A.: Late Weichselian iceberg, surface-melt and sediment production from the Eurasian Ice Sheet: results from numerical ice sheet modeling, *Mar. Geol.*, 188, 109–127, 2002.
- Skirbekk, K., Klitgaard Kristensen, D., Rasmussen, T., Koç, N., and Forwick, M.: Holocene climate variations at the entrance to a warm Arctic fjord: evidence from Kongsfjorden Trough, Svalbard, in: *Fjord Systems and Archives*, edited by: Howe, J. A., Austin, W. E. N., Forwick, M., and Paetzel, M., Geological Society, London, Special Publications, 344, 289–304, 2010.
- Skogseth, R., Haugan, P. M., and Haarpaintner, J.: Ice and brine production in Storfjorden from four winters of satellite and in situ observations and modeling, *J. Geophys. Res.*, 109, C10008, doi:10.1029/2004JC002384, 2004.
- Skogseth, R., Haugan, P. M., and Jakobsson, M.: Watermass transformations in Storfjorden, *Cont. Shelf Res.*, 25, 667–695, 2005.
- Ślubowska, M. A., Koç, N., Rasmussen, T. L., and Klitgaard-Kristensen, D.: Changes in the flow of Atlantic water into the Arctic Ocean since the last deglaciation: evidence from the northern Svalbard continental margin, 80° N, *Paleoceanography*, 20, 1–16, doi:10.1029/2005PA001141, 2005.
- Ślubowska-Woldengen, M., Rasmussen, T. L., Koç, N., Klitgaard-Kristensen, D., Nilsen, F., and Solheim, A.: Advection of Atlantic Water to the western and northern Svalbard shelf since 17,500 cal yr BP, *Quaternary Sci. Rev.*, 26, 463–478, doi:10.1016/j.quascirev.2006.09.009, 2007.
- Ślubowska-Woldengen, M., Koç, N., Rasmussen, T. L., Klitgaard-Kristensen, D., Hald, M., and Jennings, A. E.: Time-slice reconstructions of ocean circulation changes on the continental shelf in the Nordic and Barents Seas during the last 16 000 cal yr BP, *Quaternary Sci. Rev.*, 27, 1476–1492, doi:10.1016/j.quascirev.2008.04.015, 2008.
- Smedsrud, L. H., Esau, I., Ingvaldsen, R. B., Eldevik, T., Haugan, P. M., Li, C., Lien, V. S., Olsen, A., Omar, A. M., Otterå, O. H., Risebrobakken, B., Sandø, A. B., Semenov, V. A., and Sorokina, S. A.: The role of the Barents Sea in the Arctic climate system, *Rev. Geophys.*, 51, 415–449, 2013.
- Spielhagen, R. F., Werner, K., Sørensen, S. A., Zamelczyk, K., Kandiano, E., Budéus, G., Husum, K., Marchitto, T. M., and Hald, M.: Enhanced modern heat transfer to the Arctic by warm Atlantic water, *Science*, 331, 450–453, doi:10.1126/science.1197397, 2011.
- Steinsund, P. I.: Benthic foraminifera in surface sediments of the Barents and Kara seas: modern and late Quaternary applications, PhD thesis, University of Tromsø, Norway, 1994.
- Sternal, B., Szczuciński, W., Forwick, M., Zajączkowski, M., Lorenc, S., and Przytarska, J.: Postglacial variability in near-

- bottom current speed on the Continental shelf off south-west Spitsbergen, *J. Quaternary Sci.*, 29, 767–777, 2014.
- Stuiver, M. and Reimer, P. J.: Extended ^{14}C database and revised CALIB radiocarbon calibration program, *Radiocarbon*, 35, 215–230, 1993.
- Stuiver, M., Grootes, P. M., and Braziunas, T. F.: The GISP2 ^{18}O climate record of the past 16,500 years and the role of the sun, ocean and volcanoes, *Quaternary Res.*, 44, 341–354, 1995.
- Stuiver, M., Reimer, P. J., and Reimer, R. W.: CALIB 5.0. [WWW program and documentation], 2005.
- Svendsen, H., Beszczynska-Møller, A., Hagen, J. O., Lefauconnier, B., Tverberg, V., Gerland, S., Ørebæk, J. B., Bischof, K., Papucci, C., Zajączkowski, M., Azzolini, R., Bruland, O., Wiemcke, C., Winther, J.-G., and Dallmann, W.: The physical environment of Kongsfjorden-Krossfjorden, an Arctic fjord system in Svalbard, *Polar Res.*, 21, 133–166, 2002.
- Svendsen, J. I. and Mangerud, J.: Holocene glacial and climatic variations on Spitsbergen, Svalbard, *Holocene*, 7, 45–57, 1997.
- Szczuciński, W., Zajączkowski, M., and Scholten, J.: Sediment accumulation rates in subpolar fjords – impact of post-Little Ice Age glaciers retreat, Billefjorden, Svalbard, *Estuar. Coast. Shelf S.*, 85, 345–356, 2009.
- Taldenkova, E., Bauch, H. A., Stepanova, A., Ovsepyan, Y., Pogodina, I., Klyuvitkina, T., and Nikolaev, S.: Benthic and planktic community changes at the North Siberian margin in response to Atlantic water mass variability since last deglacial times, *Mar. Micropaleontol.*, 96–97, 13–28, 2012.
- Thorarinsdóttir, G. and Gunnarson, K.: Reproductive cycles of *Mytilus edulis* L. on the west and east coast of Iceland, *Polar Res.*, 22, 217–223, 2003.
- Vilks, G.: Late glacial-postglacial foraminiferal boundary in sediments of eastern Canada, Denmark and Norway, *Geosci. Canada*, 8, 48–55, 1981.
- Walczowski, W. and Piechura, J.: New evidence of warming propagating toward the Arctic Ocean, *Geophys. Res. Lett.*, 33, L12601, doi:10.1029/2006GL025872, 2006.
- Walczowski, W. and Piechura, J.: Pathways of the Greenland Sea warming, *Geophys. Res. Lett.*, 34, L10608, doi:10.1029/2007GL029974, 2007.
- Walczowski, W., Piechura, J., Goszczko, I., and Wieczorek, P.: Changes in Atlantic water properties: an important factor in the European Arctic marine climate, *ICES J. Mar. Sci.*, 69, 864–869, doi:10.1093/icesjms/fss068, 2012.
- Wanner, H., Beer, J., Bütikofer, J., Crowley, T. J., Cubasch, U., Flückiger, J., Goosse, H., Grosjean, M., Joos, F., Kaplan, J. O., Küttel, M., Müller, S., Prentice, I. C., Solomina, O., Stocker, T. F., Tarasov, P., Wagner, M., and Widmann, M.: Mid- to late Holocene climate change: an overview, *Quaternary Sci. Rev.*, 27, 1791–1828, 2008.
- Weber, M. E., Niessen, F., Kuhn, G., and Wiedicke-Hombach, M.: Calibration and application of marine sedimentary physical properties using a multi-sensor core logger, *Mar. Geol.*, 136, 151–172, doi:10.1016/S0025-3227(96)00071-0, 1997.
- Werner, K., Spielhagen, R. F., Bauch, D., Hass, H. C., Kandiano, E. S., and Zamelczyk, K.: Atlantic Water advection to the eastern Fram Strait – multiproxy evidence for late Holocene variability, *Palaeogeogr. Palaeoclimatol.*, 308, 264–276, 2011.
- Winsborrow, M. C. M., Andreassen, K., Corner, G. D., and Laberg, J. S.: Deglaciation of a marine-based ice sheet: Late Weichselian Palaeo-ice dynamics and retreat in the southern Barents Sea reconstructed from onshore and offshore glacial geomorphology, *Quaternary Sci. Rev.*, 29, 424–442, 2010.
- Witus, A. E., Braneky, C. M., Anderson, J. B., Szczuciński, W., Schroeder, D. D., and Jakobsson, M.: Meltwater intensive glacial retreat in polar environments and investigation of associated sediments: example from Pine Island Bay, West Antarctica, *Quaternary Sci. Rev.*, 85, 99–118, 2014.
- Włodarska-Kowalczyk, M., Pawłowska, J., and Zajączkowski, M.: Do foraminifera mirror diversity and distribution patterns of macrobenthic fauna in an Arctic glacial fjord?, *Mar. Micropaleontol.*, 103, 30–39, 2013.
- Wollenburg, J. E., Knies, J., and Mackensen, A.: High-resolution paleoproductivity fluctuations during the past 24 kyr as indicated by benthic foraminifera in the marginal Arctic Ocean, *Palaeogeogr. Palaeoclimatol.*, 204, 209–238, 2004.
- Zajączkowski, M., Szczuciński, W., and Bojanowski, R.: Recent sediment accumulation rates in Adventfjorden, Svalbard, *Oceanologia*, 46, 217–231, 2004.
- Zajączkowski, M., Nygård, H., Hegseth, E. N., and Berge, J.: Vertical flux of particulate matter in an Arctic fjord: the case of lack of the sea-ice cover in Adventfjorden 2006–2007, *Polar Biol.*, 33, 223–239, 2010.
- Zamelczyk, K., Rasmussen, T. L., Husum, K., Haffidason, H., de Vernal, A., Ravna, E. K., Hald, M., and Hillaire-Marcel, C.: Paleooceanographic changes and calcium carbonate dissolution in the central Fram Strait during the last 20 ka, *Quaternary Res.*, 78, 405–416, 2012.